Rapport BIPM-90/3

International comparison of activity measurements of a solution of ^{125}I (May 1988)

by G. Ratel

March 1990

Bureau International des Poids et Mesures
F-92310 SEVRES

International comparison of activity measurements of a solution of ^{125}I (June 1988)

Table of contents

Abstract

Nineteen laboratories took part in an international comparison of activity measurements of a solution of ^{125}I organized by the Bureau International des Poids et Mesures. The main features of the various methods and detectors used by the participants are described. Seven laboratories used just one method, the others employed two (seven laboratories), three (three laboratories), or even four methods (two laboratories). The final results and their uncertainties are presented in several tables and in a figure. The total range of the results is 7.2 %, or 3.5 % if one outlier is excluded. The mean value of the 38 communicated results is (1 425.6 ± 1.4) Bq mg^{-1} (weighted) and (1 429.8 ± 2.6) Bq mg^{-1} (unweighted). The uncertainty of the weighted mean value is about 0.1 % (1σ); it increases to about 0.6 % for one laboratory. For the unweighted mean the values are roughly three times higher. Two of the values reported are rather distant from the other results, but there is no known reason to exclude them. Four laboratories determined the half life of ^{125}I and reported values between 59.29 d and 59.9 d. Measurements of the half life are still going on.

1. Introduction

The isotope ^{125}I was chosen for this international comparison essentially for three reasons. First, this radionuclide is very important in medicine because of the low energy of its photon emission; patient irradiation is relatively low, so it is often used for the study of sensitive organs (as kidneys or glands); and the half life of about two months gives an advantage over the other isotopes of iodine when the effect of a treatment has to be measured over a long period of time. Second, the low photon energy of ^{125}I makes it difficult to measure this radionuclide precisely using the SIR system (International reference system for activity measurements of gamma-ray emitting nuclides); therefore, it was important to calibrate it absolutely. Finally, the reported half-life values show a large spread and it was tempting to try to arrive at a better determination of this quantity. The principal physical data concerning ^{125}I, including its decay scheme, are given in Figure 1.

In order to identify the problems associated with the measurement of this radionuclide in the frame of an international comparison and to check the feasibility of such an enterprise, the Working Group responsible for providing advice on future comparisons on behalf of Section II (Mesure des Radionucléides) of the Comité Consultatif pour les Etalons de Mesure des Rayonnements Ionisants (CCEMRI) decided to organize a trial comparison which took place in March 1987 [2]. This comparison reports four different methods of measurement. In view of the assessed uncertainties, the results communicated could be considered as satisfactory. No systematic trend was found in the distribution of the data, but the sum-peak method [3], which is the simplest to use, came out as the least precise. At the reference date of 1987-03-01, 0 h UT, the weighted mean of all the results of the trial comparison was (2 052.0 ± 3.6) kBq g^{-1}, with a total range of 32.1 kBq g^{-1}*. The highest value reported was 2 071.1 kBq mg^{-1}, and

---

* After publication of the report on the trial comparison, the AECL lowered their value for the X-X coincidence method by (0.11 ± 0.01) %. The reason for this change is the use of an improved correction for dead time in the coincidence channel. The AECL values are now
(2 057.5 ± 9.9) kBq g^{-1} for method 2, and
(2 050.2 ± 4.0) kBq mg^{-1} for the mean.
This leads for the mean values of the trial comparison to
(2 051.9 ± 3.5) kBq g^{-1} (weighted), and
(2 056.0 ± 4.2) kBq g^{-1} (unweighted),
which are very close to the values given in [2].

the lowest 2 039 kBq g^{-1}. As the analysis of the data supplied by the seven participating laboratories revealed no major problems, a full-scale comparison was agreed for the spring of 1988.

Nineteen laboratories participated in the full-scale comparison, which confirms that such an exercise is of wide interest. Organizational details are described in a circular dated March 10, 1988. The final report on the trial comparison and a report form, amended in the light of this report, were sent to participants together with the circular. As reference, the date May 15, 1988, 0 h UT was chosen. Completed forms reached the BIPM during the summer of 1988.

2. Characteristics of the solution distributed and tests of purity

At the 1987 meeting of Section II it was decided to treat ^{125}I in the same way as ^{109}Cd in a previous comparison. Three laboratories offered their services for the distribution of the radioactive solution. The NIST (formerly the NBS) offered to produce the raw material which they subsequently sent to the OMH for diluting and bottling. The LMRI received twenty-two ampoules on April 19, 1988 and dispatched 19 of them to the participating laboratories (listed in Table 1).

Each participant received a flame-sealed NBS-type ampoule containing about 3.6 g of solution. The exact masses were made known to the laboratories by the OMH and are indicated in Table 2. All later mass measurements are coherent with these data. An apparent discrepancy which appears in the data from the NIM is readily explained as this laboratory measured the mass of the remaining solution after removing about 0.4 g to prepare a dilution. On this occasion, the BIPM asked for just one ampoule because the limited sensitivity of the ionization chambers of the SIR to the photon energy of ^{125}I does not permit precise relative measurements of the activity of this radionuclide.

The solution used had a nominal activity concentration of 2.0 MBq g^{-1} (May 15, 1988) and was distributed as an aqueous solution of $5 \cdot 10^{-4}$ mol NaOH per dm^3 with 50 µg of non-active iodine in the form of KI and 50 µg of $Na_2S_2O_3$ per gram of solution.

Purity tests

In April 1988, at the request of the BIPM, the OMH performed purity tests by γ-ray spectroscopy using a small amount of the ^{125}I solution prepared for the comparison. The LMRI also carried out purity tests after receipt of the ampoules. The results expressed as a percent of ^{125}I activity (for the reference date) are listed below with the data communicated by the NIST to the OMH.

Laboratory	Impurity ^{126}I	Date of measurement
NIST	$3.18 \cdot 10^{-7}$	1988-02-22
OMH	not detected	1988-04-06
LMRI	not detected	-

We recall that $T_{\frac{1}{2}}$ (^{126}I) ≅ 13 d.

The LMRI used Ge(Li) detectors for its measurements, the detection limit being lower than $1.2 \cdot 10^{-7}$ γ s^{-1} Bq^{-1}. The volume of the OMH detector was 40 cm^3 and this laboratory covered a range of energy from 60 keV to 2.5 MeV with detection limits between $5 \cdot 10^{-7}$ and $3 \cdot 10^{-6}$ in relative value.

3. Ionization-chamber measurements and adsorption tests

Ionization-chamber measurements were carried out by eight laboratories after they had transferred and weighed the solution. Only three measured the activity of the ampoules before opening. Six results are in good agreement. The result of the NIM is high, but could be brought into line with the others by a shift of the reference date by three days. The results of the PSPKR seem much too high: perhaps the sensitivity of the ionization chamber was too low.

After the ampoules had been emptied they were rinsed twice with distilled water: the remaining activity indicates adsorption on the ampoule walls and appears to be very small. In all cases it was below $3.7 \cdot 10^{-4}$ of the original activity. Three laboratories found values of about 500 Bq for the remaining activity; for the others the reported values are up to 20 times smaller. The OMH greatly reduced the value of the remaining activity by two additional rinsings with a diluent.

Adsorption tests were made by means of γ-ray spectrometry with NaI(Tl) detectors (four laboratories, of which two used a well-type crystal), high-purity germanium detectors (four laboratories) or Ge-Li detectors (one laboratory). For these measurements the NPL and the PSPKR used ionization chambers and the NIM employed the liquid-scintillation method. All these data are assembled in Table 3.

4. Source preparation

In describing work on this nuclide it is convenient to treat source preparation according to the method used for measuring the activity. This section is divided into three parts: sources for electron counting, sources for γ- and X-ray counting and sources for liquid-scintillation counting. Relevant data are given in Tables 4 to 6.

a) Sources for electron counting

Six laboratories out of nineteen performed measurements for which the electron count rate was necessary. Almost all sources were made from a dilute solution deposited on a metal-coated support. The NRC performed directly application of the master solution. Dilution factors ranged from about 3 (NPL) to 42 (CBNM). In order to avoid the risks of sublimation of ^{125}I, and therefore of contamination of the β counter, the NPL and the VNIIM sandwiched their sources. In all cases a wetting agent (catanac SN for the AECL, NPL and NRC) or a seeding agent (insulin for the VNIIM and $AgNO_3$ for the ETL) was added to the solution. However, most laboratories used $AgNO_3$ as a stabilizer for volatile iodine compounds. The sources were dried under ambient laboratory air conditions in the case of the AECL, CBNM, NPL and VNIIM. The ETL put the sources in a silica gel dessicator and the NRC dried them in warm air. All sources were in the same mass range, namely 10 to 40 mg for the diluted solution and 10 to 23 mg for the master solution. The number of sources used was also about the same (from six for the AECL to ten for the NPL). The mass measurements were performed in most cases with a Mettler M5 balance, except for the VNIIM which used a balance of Russian origin. Details of source preparation are given in Table 4.

b) Sources for X- and γ-ray counting

Most participants prepared sources for X- and γ-ray counting. The laboratories counting electrons used the same dilutions as just described but some changed the support of the sources (e.g. polyester tape instead

of VYNS foils in the case of the AECL). Six laboratories (IEA, KSRI, NAC, NRC, PTB for method 4 and VNIIM) used undiluted solutions. The films were metal-coated by just two laboratories (NRC and PTB). The NIM covered its sources with a thick layer of Al on both sides (8.3 mg cm^{-2}) to absorb the conversion electrons. Three laboratories sandwiched their sources (AECL, NAC and UVVVR) so as to avoid sublimation of the substrate. The drying conditions were comparable with those used for electron counting. The LMRI and the NAC accelerated the drying process using an infrared lamp. Some special treatments are summarized in Table 5. The NIST noted that $AgNO_3$ is effective in immobilizing the iodine but produces silver X rays which may confuse the analysis. To avoid these difficulties they applied an ion-resin paper, an approach which has shown its effectiveness over many years (particularly in the case of ^{129}I).

Dilution factors showed a larger spread than those used for electron counting ranging from 1.13 (NIM) to 76.8 (NIST). Source masses ranged from 2 mg (NAC) to 151 mg (ENEA), but in most cases the mass was below 50 mg. Mettler balances were the most frequently used for the measurement of the drop masses. The NIM and the VNIIM worked with apparatus constructed in their own countries and the UVVVR used a Sartorius balance. All sources were in solid form, except those of the OMH and some of the NAC which were liquid. The number of sources measured was usually below fifteen, but three laboratories used significantly more: CNEN (20), ENEA (25) and NIST (33). Further details are given in Table 5.

c) Sources for liquid-scintillation counting

The NAC is the only laboratory which used the liquid-scintillation method. The dilution factor was 2.045 and the seven sources were prepared in 20 ml glasses with about 45 mg of solution to which a scintillation solution of commercial type was added. Table 6 summarizes the characteristics of these sources.

5. Detectors for proportional and photon counting

The main data concerning the different types of detectors are compiled in Tables 7, 8 and 9. However, it is worth emphasizing some particular device characteristics.

a) Proportional counter (PC)

Five laboratories (AECL, ETL, NPL, NRC and VNIIM) used a proportional counter. In all the methods used by the NRC (three) and the NPL (one) this type of detector is necessary. The proportional counters were of the gas-flow type and most used Ar + CH_4 in the proportion 9 to 1. At the NPL, CH_4 was also used. All the counters worked at atmospheric pressure. In most cases, the walls were made of metal, gold-coated in the case of the ETL. However, the AECL used polyester films for the bottom and top walls, and the NPL inserted silver-coated perpex pieces to define the counting volume. A schematic view of the AECL counter is given in reference [4] and a sketch of the NPL measuring equipment is shown in Figure 2. All detectors were of about the same height, but that of the NPL was roughly half as high as the others. The useful volume of the VNIIM detector was much larger than average. The ETL and the NRC worked at constant high voltage and varied the discrimination level from 0.5 keV to 2 keV (ETL) or from 60 mV to 460 mV (NRC). The AECL varied the high voltage in order to produce an effective change in the discrimination level. The NPL and the VNIIM did the same, choosing the discrimination level in the centre of the plateau.

The AECL, the NRC and the VNIIM worked with a dead time of about 2 μs, whereas the NPL used a lower value (1.27 μs) and the ETL a larger one (7.85 μs). Data concerning the anodes can be found in Table 7.

b) Scintillation detectors for X- and γ-ray counting

All participants used a scintillation detector to measure the activity of the iodine solution. Except for CBNM, which made use of a CsI(Tl) sandwich spectrometer described in [6], the detectors were of the NaI(Tl) type. Several laboratories (CBNM, ENEA, ETL, NIST, OMH and PSPKR) determined the activity with a well-type NaI(Tl) detector. The distance between source and detector was kept constant and generally chosen below 15 mm, although four laboratories (BIPM, ETL, LMRI and NRC) used a greater separation. When an efficiency extrapolation was necessary, the counter-source distance varied significantly, namely from 0.3 mm (for the PSPKR) to 150 mm (for the KSRI and the PTB). The solid angle had a value close to 4π for all well-type detectors and also for the CsI(Tl) sandwich spectrometer. All participants worked with external dead times, except the CBNM (one method), and the ETL which performed live-time measurements with a multichannel analyzer. The NAC performed all counting using timer/scalers, and applied dead time corrections. The dead times were all independently determined prior to the actual measurement of the activity. The adopted dead times were usually between 1.5 μs (VNIIM) and 5.9 μs (CBNM), the most

common values being close to 5 μs. Some laboratories, however, adopted much larger dead times: ETL (8 μs), CBNM method 5 (10.6 μs), LMRI (20 μs) and NPL (19.9 μs). The NAC used the value of 54 μs as the effective dead time for the sum-peak X-ray events of method 6. Other characteristics of the scintillation counters are given in Table 8.

c) Semi-conductor detectors for photon counting

In the semi-conductor category the choice of detectors was less uniform. Two laboratories (NRC and PTB) used Si(Li) detectors. The others worked with a pure Ge detector (AECL), a pure Ge-N-type detector (NPL) or Ge(Li) detectors (NRC). All semi-conductor detectors were covered with a metallic window. This was a thin foil of beryllium in the case of the AECL, the NRC and the PTB; the NPL used an Al foil (1 mm) for the same purpose. The distance between source and detector was commonly about 40 mm. The PTB kept its sources at 8.5 mm from the crystal. Two laboratories (AECL and NRC) used a value of about 2 μs for the dead time. The NRC worked with an extended dead time of 5.06 μs for the anticoincidence channel, whereas the NPL took a larger value (19.9 μs). Further details can be found in Table 9.

6. Coincidence and anticoincidence counting

The data describing the coincidence and anticoincidence counting are assembled in Table 10. They do not lend themselves to a clear grouping, but it may be noted that the coincidence resolving time τ_R is always between 0.5 and 1.0 μs. Only two laboratories worked with a somewhat different value: the BIPM took $\tau_R = 0.239$ μs and the VNIIM used $\tau_R = 2.0$ μs in one of their methods. In most cases the dead times and coincidence resolving times were determined by the two-oscillator method [7].

Use was also made of a calibrated oscilloscope (KSRI), which at the NPL was associated with a tail-pulse generator. The VNIIM measured the dead time by means of the source-pulse method. They obtained the resolving time by looking at the delayed coincidence curve, whereas the NIM used accidental coincidences. The CNEN measured the accidental coincidence rate with uncorrelated random pulses. For additional details, see Table 10.

7. Counting data for the different methods

The main counting data corresponding to the different methods used by the participants are listed in Table 11. One can see that the typical count rates generally remain below 3 000 s^{-1}. The lowest count rate, measured by the NAC when applying the liquid-scintillation method, was 34 s^{-1} and corresponded to the rate of the sum-peak X rays in coincidence with an electron rate of 26 000 s^{-1}. At the BIPM and the CNEN additional low count-rate sources (80 s^{-1} and 50 s^{-1}, respectively) were used. Elsewhere, sources delivering count rates of 20 000 s^{-1} or more were measured: at the PTB (20 000 s^{-1}), the NAC (21 000 s^{-1} and 26 000 s^{-1}) and the NRC (35 000 s^{-1}). The count durations for individual measurements were adapted to the emission rate of the sources in order to obtain good statistics; it ranged from 200 s for the highest count rate to 15 000 s for the lowest one. The background rates remained quite low, especially at the PTB where a value of 0.04 s^{-1} was obtained with a Si(Li) detector. The number of measured sources was often smaller than 15, but five laboratories used more (up to 33 at the NIST).

All measurements were performed between May 3 and August 29, 1988, but, as requested, most laboratories succeeded in measuring their sources at close to the reference date. This helped to reduce the effect of uncertainty in the half life on the precision of the submitted results. An unexpected delay in the distribution of the sources perturbed the planning at some laboratories and led to a wider spread in the dates of measurement than had been intended.

8. Activity measurements, description of the methods used

In this section we give details of the different methods used by the laboratories for measuring activity. The order in which the methods are analyzed is arbitrary and does not imply a classification. Four methods were used for the trial comparison, their numerical order being given in [2]. The order adopted there is repeated in Tables 4 to 15. Methods 5 to 8 have been used by just one laboratory.

a) Method of Eldridge and Crowther (method 1) [3]

Thirteen laboratories out of nineteen used the Eldridge and Crowther method. Its principal benefit is its simplicity because it requires only one detector. This, in most cases, was of the NaI(Tl) type. The NIST and the OMH used this method twice. The former laboratory performed its

measurements once close to the originally chosen reference date and the second time about June 15. The set of data corresponding to the second measurement is referred to as 1bis. The AECL employed a Ge detector and the PTB a Si(Li) detector.

As NaI(Tl) detectors have poor resolution, events with similar energies are not resolved and so form a single peak. Events due to photons which are emitted almost simultaneously are summed and give rise to a second peak in the ^{125}I spectrum. Figures 3.1 to 3.3 show typical spectra obtained with method 1. The area of the two peaks (in the case of a spectrum obtained by means of a NaI(Tl) detector) or of the peaks belonging to a well-defined energy range (in the case of a Ge detector (AECL) or a Si(Li) detector (PTB)) can be used for evaluation of the activity of the source. If we denote the contents of the first peak (corresponding to the single events) as A_1, and the contents of the second peak (corresponding to the sum peaks) as A_2, the activity is given by the relation

$$N_o = \frac{P_1 P_2}{(P_1 + P_2)^2} \frac{(A_1 + 2A_2)^2}{A_2}, \qquad (1)$$

where $P_1 = P_K \omega_K$ and $P_2 = \frac{\alpha_K \omega_K + 1}{1 + \alpha_T}$ are respectively the probability per decay of K X-ray emission in the electron capture transition and the sum of the emission probabilities per decay of the 35 keV gamma ray and the K X-ray arising from internal conversion. Estimates of these two probabilities can be found in Table 12 and in most cases are calculated using the nuclear constants given in [1]. The main weakness of this method lies in the difficulty of determining the exact contributions of the two peaks in the region of overlap and of separating the single event peak from the noise which disturbs the spectrum at low energy.

To avoid these cumbersome problems, the PTB, as already mentioned, used a high resolution Si(Li) detector. A typical spectrum obtained by this laboratory is shown in Figure 4. The region 1, corresponding to the range of energy between 20 keV and 38 keV, contains pulses from primary photons produced by electron capture in the parent nuclide ^{125}I as well as pulses from primary photons in and following the transition from the excited level to the ground level in the daughter nuclide ^{125}Te. In region 2, ranging from E = 38 keV to 69 keV, coincident events, resulting from the sum of single pulses, are registered.

The activity is given by a formula similar to (1), specifically

$$N_o = 0.9981 \frac{[S_1 + 2(S_2 + \delta S_1)]^2}{4 S_2} . \qquad (2)$$

The meaning of the quantities appearing in (2) is shown in Figure 4.

To reduce the effect of unwanted pulses coincident with ^{125}Te L radiations, a 35 μm thick absorber foil of aluminium was placed between the active source and the detector.

b) Method of J.G.V. Taylor (method 2) [8]

The Taylor method, employed by 11 laboratories, was that used most frequently following method 1. Its application requires two high-efficiency detectors (normally NaI(Tl) detectors) facing each other. They collect two similar disintegration spectra and each channel is gated to accept all sum-coincidence events. Spectra obtained with this method are shown in Figure 5.

If N_1 and N_2 are the numbers of events registered in the gate, including both the singles peak and the sum peak on each channel, and N_c is the number of coincidence events occurring in the two channels, the activity of the source can be calculated by means of the expression

$$N_o = \frac{4K}{(1+K)^2} \left[N_1 + \frac{N_c(1 - N_c/2N_2)}{2(1 - N_c/2N_1)}\right] \left[N_2 + \frac{N_c(1 - N_c/2N_1)}{2(1 - N_c/2N_2)}\right] \frac{1}{2N_c} , \qquad (3)$$

where $K = \frac{1 + \alpha_K \omega_K}{P_K \omega_K (1+\alpha_T)}$, the ratio of detection probabilities per disintegration, is supposed equal for both counters.

If N_1 and N_2 are the registered events in the singles peak, the formula quoted above has to be modified to

$$N_o = \frac{4K}{(1 + K)^2} \left[N_1 + N_c \frac{(1 - N_c/N_2)}{(1 - N_c/N_1)}\right] \left[N_2 + N_c \frac{(1 - N_c/N_1)}{(1 - N_c/N_2)}\right] \frac{1}{2N_c} . \qquad (4)$$

c) 4πe-X coincidence-efficiency extrapolation method (method 3) [4]

The 4πe-X coincidence-efficiency extrapolation method was used by four laboratories (AECL, ETL, NPL and VNIIM). In order to detect the conversion electrons emitted by ^{125}Te a proportional counter was used and the X and

γ rays were detected by scintillation detectors. The activity of the source is then obtained by the well-known formula

$$N_o = \frac{N_\beta^* N_\gamma^*}{N_c^*} , \tag{5}$$

where N_β^* and N_γ^* are the true count rates after correction for dead times, coincidence-resolving times and background. The expressions for N_β^* and N_γ^* (in the case of the AECL for example) are given below.

$$N_\beta^* = \frac{N'_\beta}{1 - \tau_\beta N'_\beta} - B'_\beta , \tag{6}$$

$$N_\gamma^* = \frac{N'_\gamma}{1 - \tau_\gamma N'_\gamma} - B'_\gamma , \tag{7}$$

$$N_c^* = \frac{\left[N'_c - (\theta_\beta + \theta_\gamma) N'_\beta N'_\gamma\right] (2 - \tau_\beta N'_\beta - \tau_\gamma N'_\gamma)}{\left[2-\tau_\beta N'_\beta-\tau_\gamma N'_\gamma+2\tau N'_c - 2(\theta_\gamma N'_\beta+\theta_\beta N'_\gamma) + 2\delta(N'_\beta-N'_\gamma)\right] (1-\tau_\beta N'_\beta)(1-\tau_\gamma N'_\gamma)} - B'_c, \tag{8}$$

where the primes (') designate observed rates, θ refers to the coincidence resolving time, τ is the dead time, δ is the delay mismatch between the two channels and B refers to the background rates. To obtain the activity N_o the quantity $N_\beta^* N_\gamma^* / N_c^*$ is evaluated and plotted against $N_\gamma^*/N_c^* - 1 = (1-\varepsilon_\beta)/\varepsilon_\beta$. The extrapolation for $\varepsilon_\beta = 1$ then gives the activity of the solution. Figure 6 shows some examples of such an extrapolation. Not all users of method 3 employed formula (8).

d) Photon-photon coincidence counting and efficiency-extrapolation method (method 4) [9]

The photon-photon coincidence counting and efficiency-extrapolation method, like method 2, is based on the use of two NaI(Tl) detectors mounted so as to face the source, but in such a way that the distance between each crystal and the source can be varied [9]. Consequently, systematic effects can be studied. Starting from the equations written down by Taylor in the case of method 2, and with the notation used in paragraph 8b, one obtains the following relation

$$\frac{N_1 N_2}{2N_c} = N_o \frac{(1 + K)^2}{4K} \left\{1 - \frac{K}{1 + K} (\varepsilon_1 + \varepsilon_2) + \frac{K^2}{(1 + K)^2} \varepsilon_1 \varepsilon_2\right\} , \tag{9}$$

where

$$\varepsilon_1 = \frac{(1 + K)}{2K} \frac{N_c}{N_2} \left[1 - \frac{1}{2} \frac{N_c}{N_1}\right] / \left[1 - \frac{1}{4} \frac{N_c^2}{N_1 N_2}\right]$$

and

$$\varepsilon_2 = \frac{(1+K)}{2K} \frac{N_c}{N_1} \left[1 - \frac{1}{2} \frac{N_c}{N_2}\right] / \left[1 - \frac{1}{4} \frac{N_c^2}{N_1 N_2}\right] .$$

The coefficient K is defined in paragraph 8b. Minor discrepancies in K which appear among the participants arise from the use of different nuclear data but do not contribute significantly to the uncertainty of N_o.

If the efficiencies ε_1 and ε_2 are varied by changing the distance between source and detector, a value for expression (9) at zero efficiency may be obtained by extrapolation and the activity of the source is deduced by linear regression from

$$y(x) = \frac{N_1 N_2}{2N_c} = N_o \frac{(1+K)^2}{4K} (1 - x) \qquad (9')$$

with $x = \frac{K}{1+K} (\varepsilon_1 + \varepsilon_2) - \frac{K^2}{(1+K)^2} \varepsilon_1 \varepsilon_2$.

Six laboratories (CBNM, CNEN [10], KSRI, NAC, PSPKR and PTB) used method 4. Some data relative to this method can be seen in Figure 7. An example of an extrapolation curve obtained by the NAC is shown in Figure 8.

e) Method of B. Denecke (method 5) [6]

The method of B. Denecke (used at the CBNM) is essentially based on a 4π-CsI(Tl) sandwich spectrometer which permits work with X- and γ-ray efficiencies, as well as conversion-electron and Auger efficiencies, close to unity ($\varepsilon_\gamma = \varepsilon_{KX} = 0.999\ 5$ and $\varepsilon_{KA} = \varepsilon_{ce} = 0.965$). Almost all events can be registered, which is why the method is also referred to as the "total counting method".

The activity is evaluated using the expression

$$N_{tot} = N_o \{P_{ce} + P_{IT} - P_{ce} P_{IT}\} , \qquad (10)$$

with the probabilities $P_{ce} = P_K \{\omega_K \varepsilon_{KX} + a_K \varepsilon_{KA}\}$ for conversion electrons and $P_{IT} = \frac{1}{1+\alpha} \{\alpha_K (\omega_K \varepsilon_{KX} + a_K \varepsilon_{KA}) + \alpha_L + \varepsilon_{ce} + \varepsilon_\gamma\}$ for isomeric transitions. Experimental results corresponding to this method are shown in Figure 9.

f) 4π(LS)e-X method (method 6) [11]

The 4π(LS)e-X method, used at the NAC, is identical with method 3, except that the proportional counter is replaced by a liquid scintillation system and the variation of the counting efficiency is obtained by means of a threshold discrimination. These differences seem to justify a distinction between the two methods.

During the ^{125}I measurements a window was set on the X-ray channel so as to select only true sum-peak events. The efficiency was varied between 0.45 and 0.71. A separate check showed minimal adsorption of ^{125}I on the walls of the source cell. Typical spectra, and an example of an extrapolation curve, are given in Figure 10.

g) 4π(PC)e photon-anticoincidence method (method 7) [12]

The NRC used the 4π(PC)e photon-anticoincidence method which is based on live-time measurements. The anticoincidence counts (N_β) are related to the source disintegration rate N_o by the following equation taken from Baerg [13],

$$N_\beta = N_o + A_1 Y_1 / N_{\gamma_1} + A_2 Y_2 / N_{\gamma_2} ,$$

where A_1 and A_2 are coefficients obtained by a fitting procedure, Y_1 and Y_2 are the anticoincidence rates, and N_{γ_1} and N_{γ_2} are the γ-ray monitor rates. Typical data are shown in Figure 11.

h) 4π(PC)e photon-coincidence method (method 8)

The 4π(PC)e photon-coincidence method was used only at the NRC and is described in [7]. The activity is again determined by extrapolation of the quantity $N_\beta N_\gamma / N_c$ to the condition that the β-counting efficiency approaches unity. A spectrum is shown in Figure 12.

9. Corrections used for evaluating the results

The corrections applied by the different laboratories for evaluating the results are listed in Table 12. Some of them depend on the method used, but as a rule the count rates were corrected for background, dead times and radioactive decay during the measurements. In the following we indicate the corrections which were applied for each method mentioned in section 8. The corresponding numerical values of the nuclear data used by the laboratories in calculating the activity are given in Table 12.

Apparently, most laboratories used the radionuclide tables of the LMRI [1]; only the value of the CBNM for ω_K was slightly lower (with negligible effect on K).

a) Method 1.- The ENEA performed a linear extrapolation of the "tails" for separating the singles and sum peaks. The accidental summing in the sum peak was accounted for by extrapolation to zero count rate. The ETL took into account the effects due to pile-up pulses in the pulse-height distribution and corrected measurements by extrapolating to zero source strength. The NIST (method 1) computed a correction for the sum-peak tail as 1.2 times the semi-logarithmic tail. For method 1bis an extrapolation to zero count rate was performed. This procedure was also applied by the PSPKR. The OMH evaluated graphically a correction for the contribution of the tail of the two peaks and an extrapolation to zero count rate was made to eliminate the effect of accidental summing.

b) Method 2.- The AECL corrected the X-X coincidence rates for accidental coincidences. The CBNM and the UVVVR used the Cox-Isham formula [14] to perform dead-time corrections. Moreover, the CBNM applied corrections for foil adsorption, self absorption for electrons and, although they remain quite small, corrections for the solid angle. The NAC used the Bryant formula [15] for correcting the coincidence count rate.

c) Method 3.- The AECL corrected the individual e-X coincidence rates for delay mismatch and accidental coincidences. The ETL estimated the correction due to accidental coincidences to be 10 % using the Campion formula [16]. The NPL applied the Cox-Isham formula (modified by Smith) [17] to correct for dead time and resolving time.

d) Method 4.- The CBNM and the PTB corrected the measurements by means of the Cox-Isham formula [14]. The NAC applied the formula of Bryant [15] for correcting the coincidence count rate.

e) Method 5.- The CBNM corrected in the same way as for methods 2 and 4. The self absorption and the foil absorption for electrons as well as the solid-angle contribution were also taken into account. It should be noted that in this case the correction due to the peak tailing was taken as an exponential below 7.4 keV and its value was between 0.2 % and 0.4 %. The background correction was as large as 1.4 %.

f) Method 6.- The NAC corrected for dead time and coincidence-resolving time (0.47 %). In addition, satellite pulses were accounted for (0.12 % to 0.23 %).

10. Uncertainties

As in previous comparisons all participants assessed values for the uncertainty components. This time they also provided information explaining how they arrived at their values.

The various contributions to the uncertainty are described in detail in the somewhat cumbersome Table 13. Two kinds of uncertainties can be considered. Some are common to all methods: important among these are those due to counting statistics, weighing, dead time, background and timing. Among the others, which depend more or less on the method used, are the uncertainties due to the evaluation of N_1 and N_2, extrapolations and accidental coincidences. Superficially, it appears that method 1, contrary to what would be expected from the trial comparison, does not lead to much larger uncertainties than the other methods. Most laboratories assessed their total uncertainties at about the same value. Exceptions are the AECL for which the uncertainties are very small (0.06 % and 0.05 % for methods 2 and 3) and the PSPKR which arrived at uncertainties of about 1 % (from 0.90 % for method 2 to 1.20 % for method 1). The uncertainty assessment of the AECL appears to be justified by the fact that this laboratory performed a considerably larger number of measurements than the others and that the results of the three methods used are very consistent.

Table 14 is restricted to the main uncertainty components of the final result for a given laboratory and to the method given. The contributions are listed in the inverse order of their magnitude, and the total uncertainty is given for comparison.

- In the case of method 1 the tail extrapolation (CNEN, NIST, OMH and PTB), the peak separation (CBNM and OMH) and the gate setting (ETL and UVVVR) are the major contributions to the uncertainty. Other laboratories call attention to data fitting (NAC), and sum-peak effects (which disappear when the window includes only singles). For the AECL and the CBNM the contributions of the counting statistics are the most important, but for the ENEA the decay-scheme corrections were dominant. The PSPKR found that weighing, dead time and other effects (not explained) led to 0.6 % uncertainty in each case.

- For method 2 the main contributions came from counting statistics for the AECL, CBNM and CNEN, decay-scheme corrections for the IEA, LMRI and NAC, and half-life corrections for the BIPM, KSRI and UVVVR which also reported a non-negligible contribution from the dilution. For the PSPKR, weighing gave the largest component to the uncertainty; the VNIIM noted that other effects (not explained) played the same role.

- In the case of method 3, the main contribution to the combined uncertainty was considered to be counting statistics (AECL), extrapolation (ETL and NPL) and weighing (PSPKR). The VNIIM mentioned other effects but gave no details.

- For method 4 the CBNM reported that counting statistics played a decisive role; the NAC found that the main contribution came from the decay-scheme corrections, while the PTB mentioned problems connected with source preparation (chemical effects and precipitation) as the main source of uncertainty.

- In the case of method 5 the weighing and the tail extrapolation were mentioned by the CBNM as the main contributions to the total uncertainty.

- For method 6 (used by the NAC) the fitting of data and, to a lesser extent, the counting statistics gave the largest contributions.

- For methods 7 and 8 the NRC reported that the spread in the values observed after changing experimental conditions, such as the counting gas or the gamma-window setting (in order to include the sum peak), and the efficiency extrapolation were the main sources of uncertainty.

All the uncertainty components, considered as approximations of the corresponding standard deviations, are added in quadrature [18] when uncorrelated. No distinction between type A and type B was requested in this comparison.

The AECL made a special effort to obtain very small statistical uncertainties, thus permitting a critical comparison of the methods used (1, 2 and 3). The relative discrepancy between methods 2 and 3 was found to be (0.13 ± 0.07) % when the decay-scheme-dependent factor K was assumed to be free of error. By a small change (-0.06 %) of the value of this factor, agreement of the two values within the quoted combined uncertainties could be achieved. The results of the three methods can therefore be considered as consistent and there is no evidence for a real difference between them (at least at the present level of uncertainty). However, the AECL also mentioned that for method 1 the results obtained with an NaI(Tl) detector were higher by (1.5 ± 0.3) % than those obtained with a Ge detector. This discrepancy may result from the difficulty in separating singles and sum peak in the NaI(Tl) spectrum. Hence, the use of an appropriate detector might improve the precision of method 1.

11. Final results

All the reported values of the activity concentration and their combined uncertainties, corrected to the reference date (1988-06-15, 0 h UT), are assembled in Table 15, but in Figure 14 just one value per method and per participant is represented. When a laboratory gave several results for one method, a weighted mean was computed and plotted in Figure 14 (NIM and UVVVR). In the case of the OMH, only the value obtained close to the reference date was considered in the evaluation of the mean value and plotted in Figure 14. For the NIST two values, although obtained with the same method, were taken into account because independent teams were involved.

The mean value $\bar{x}$ and its standard deviation $s(\bar{x})$ were evaluated using (for n data $x_i \pm s_i$)

$$\bar{x} = \frac{\sum_{i=1}^{n} g_i x_i}{\sum_{i=1}^{n} g_i} \quad \text{and}$$

$$s^2(\bar{x}) = \frac{\sum_{i=1}^{n} g_i (x_i - \bar{x})^2}{(n-1) \sum_{i=1}^{n} g_i} ,$$

where $g_i = 1/s_i^2$ when statistical weights are applied; otherwise $g_i = 1$.

The AECL used three methods and found values consistently about 1.5 % lower than the average of the values found by other participants. To investigate this the AECL group prepared additional sources from the original solution and found values (1.45 ± 0.13) % higher than the mean of their previous results. These new values are in good agreement with those of the other laboratories. The discrepancy has not been explained but it is believed to indicate a problem with the stability of the solution. The AECL pointed out that similar problems have been already reported in the past with some iodine solutions. In fact, the possible existence of a sampling problem does not invalidate the statement that the three methods of measurement used at the AECL are consistent within 0.1 % because all the measurements were performed with the same set of sources. As smaller

uncertainties were assessed, especially for methods 2 and 3, these lower values affect the final results when weights are used. Another laboratory (KSRI) arrived at an activity concentration which is clearly lower than both the mean of all measurements and the mean of the results obtained by method 4. The difference is about 5 % in each case.

In all cases we have considered each method separately, even when the laboratory (AECL and UVVVR, see Table 15) reported only a mean value.

The following points can be made about the results listed in Tables 16, 17 and 18. First, the weighted and unweighted mean values obtained by methods 1 and 2 are very close (the largest discrepancy is 0.26 %). The uncertainties are also very similar. The agreement with the mean values for all methods and all laboratories reported in Table 16 is also very good. On the other hand, methods 3 and 4 show a larger dispersion of results and uncertainties. The small uncertainty assessed by the AECL in the case of method 3 is responsible for the small value of the uncertainty associated with the weighted mean. However, if there was a sampling problem, the precision of the individual measurements is not an indication of their accuracy and it is preferable to consider only the unweighted mean of all results in assessing the quality of the comparison. As can be seen from Table 18, the omission of the ETL value (method 3) or the KSRI value (method 4) does not change the discrepancy between the different weighted mean values. On the contrary, it improves the agreement between the weighted mean values obtained by methods 1, 2 and 4. In the case of method 4 the weighted and unweighted mean values are quite identical. Finally and under the same conditions, the mean values obtained for all methods remain almost unchanged (Table 17).

The results of this international comparison cover a total range of 7.23 %. The deviations of the lowest and the highest values from the weighted mean are - 4.72 % and 2.50 %, respectively. As currently we have no good reason to exclude the values obtained by the KSRI (1 358 kBq g^{-1}, method 4) and the ETL (1 461 kBq g^{-1}, method 3) the present results show a much larger spread than those of the trial comparison [2]. This was to be expected given the increase in number of participants. In this context we should mention, as pointed out by the PTB, that the KSRI obtained their value using a very thin detector (1 mm high), which could have led to the recorded discrepancy. Despite the spread of the measurements, the mean values (Table 16) have relative uncertainties which are clearly smaller than those reported in [2].

12. Determination of the half life of ^{125}I

Only four laboratories (AECL, ENEA, LMRI and NAC) made a determination of the half life of ^{125}I during the comparison. Their results are given in Table 15. The AECL found a value of (59.29 ± 0.07) d, based on three sources which had already been measured during the trial comparison in March 1987. The ENEA performed measurements from May 6 to June 23, 1988 and reported a value of (59.38 ± 0.03) d. The LMRI made measurements from May 5 to June 29, 1988. From the combined data a half life of (59.9 ± 0.11) d has been calculated, but work continues with the aim of improving this result. Using the solution supplied by the OMH for the comparison, the NAC estimated the half life and obtained a value of (59.40 ± 0.05) d, which is in very good agreement with the value adopted for the comparison. Further information can be found in ref. [19].

Two laboratories had measured the half life of ^{125}I during the trial comparison. The PTB obtained a value of (59.39 ± 0.02) d [20]. The NRC used an ionization chamber and performed measurements over a period of 346 days; a value of (59.26 ± 0.03) d was found.

13. Conclusion

Eight different methods have been used by 19 participating laboratories to measure the activity concentration of a ^{125}I solution. Although the results of this full-scale comparison show a scatter which is larger than that obtained in a trial comparison, the mean value is more accurate. Two results seem to deviate somewhat from the others and remain unexplained. All results were evaluated supposing the half life of ^{125}I to be (59.4 ± 0.5) d, with the exception of the LMRI which preferred to use its own value. As far as possible, measurements were made close to the reference date so as to reduce the dependence of the measurements on the supposed value of the half life. Separately, four laboratories made measurements of the half life with results close to the value recommended for the present international comparison.

Acknowledgments

The BIPM is pleased to express its gratitude to those national laboratories whose generous contributions have made this international comparison possible. Especial thanks are due to the NIST for supplying the radioactive solution, the OMH for preparing and bottling it, and the LMRI for the dispatching.

I wish to thank all those who participated for their efforts and for the high quality of the work performed. The detailed description of their measurements has been the indispensable basis for the present report. Thanks are also due to all participants for their numerous suggestions which have led to an improvement of the preliminary report.

I am very grateful to several members of the staff of the BIPM, in particular Dr. J.W. Müller for his constant interest in the measurements of ^{125}I performed at the BIPM, for the careful reading of the manuscript and for suggesting many improvements to the text, Dr. D.A. Blackburn for many linguistic remarks, P. Bréonce, C. Colas and C. Veyradier for their active participation in the comparison and - last, but not least - D. Müller for typing the text.

Table 1 - List of the participants

		Names of the persons who carried out the measurements
AECL	Atomic Energy of Canada Limited, Chalk River, Canada	R.H. Martin
BIPM	Bureau International des Poids et Mesures, Sèvres, France	P. Bréonce, C. Colas, G. Ratel, C. Veyradier
CBNM	Central Bureau for Nuclear Measurements, CEC-JRC, Geel, Belgium	E. Celen, B. Denecke, D.F.G. Reher
CNEN	Comissão Nacional de Energia Nuclear, Rio de Janeiro and São Paulo, Brazil	M.S. Dias, A. Iwahara, M.F. Koskinas, M.-H. Maréchal, C.J. da Silva
ENEA	Laboratorio di Metrologia delle Radiazoni Ionizzanti ENEA-CRE Casaccia, Rome, Italy	P. de Felice, C. Zicari
ETL	Electrotechnical Laboratory, Ibaraki, Japan	Y. Hino, Y. Kawada
IEA	Instytut Energii Atomowej, Swierk, Poland	A. Chylinski, T. Radoszewski, T. Terlikowska-Drozdziel
KSRI	Korea Standards Research Institute, Taejon, Korea	Tae Soon Park, Pil Jae Oh, Sun-Tae Hwang
LMRI	Laboratoire de Métrologie des Rayonnements Ionisants, Saclay, France	P. Blanchis, J. Bouchard
NAC	National Accelerator Centre, Faure, South Africa	B.R.S. Simpson, B.R. Meyer
NIM	National Institute of Metrology, Beijing, People's Republic of China	Li Fen, Li Zuo-qian
NIST	National Institute of Standards and Technology, Gaithersburg, USA (formerly NBS)	C. Ballaux, Dan Golas, Don Gray
NPL	National Physical Laboratory, Teddington, United Kingdom	A.S. Munster, D. Smith

OMH	Országos Mérésügyi Hivatal, Budapest, Hungary	M. Csikos, Gy Horvath, A. Szörényi, A. Zsinka,
PSPKR	Pusat Standardisasi dan Penelitian Keselamatan Radiasi, Jakarta, Indonesia	W. Gatot, Nazaroh, Pujadi, Sudarsono, Sunaryo
PTB	Physikalisch-Technische Bundesanstalt, Braunschweig, Federal Republic of Germany	U. Schötzig, H. Schrader, H. Siegert
UVVVR	Ustav pro vyzkum, vyrobu a vyuziti radioisotopů, Prague, Czechoslovakia	J. Formankova, J. Plch
VNIIM	Institut de Métrologie D.I. Mendéléev, Leningrad, USSR	A.A. Konstantinov, T.E. Sazonova, S.V. Sepman

Table 2 - Mass measurements of solution

Laboratory	Ampoule number	Mass of solution (g)*		
		indicated by OMH	determined by laboratory	
AECL	OMH-8 857	3.603 9	3.593 9	(1)
BIPM	OMH-8 858	3.603 2	3.594 2	
CBNM	OMH-8 859	3.603 6		
CNEN	OMH-8 863	3.604 4	3.588 0	
ENEA	OMH-8 860	3.603 8	3.602 5	
ETL	OMH-8 862	3.605 7	3.605 4	
IEA	OMH-8 861	3.605 0	3.604 9	
KSRI	OMH-8 864	3.605 8		
LMRI	OMH-8 865	3.603 9	3.603 8	
NAC	OMH-8 866	3.603 8	3.604 6	
NIM	OMH-8 868	3.603 7	3.188 9	(2)
NIST	OMH-8 867	3.603 1		
NPL	OMH-8 869	3.604 3	3.602 4	
NRC	OMH-8 870	3.604 5		
OMH	OMH-8 880	3.602 9	3.595 8	
PSPKR	OMH-8 874	3.605 8	3.566 0	
PTB	OMH-8 872	3.603 7	3.604 2	
UVVVR	OMH-8 873	3.604 9		
VNIIM	OMH-8 875	3.602 8		

* Corrected for air buoyancy.

(1) This value is the sum of the mass of active solution taken from the ampoule, i.e. (3.590 57 ± 0.000 04) g, and the residual mass found in the ampoule (0.003 3 ± 0.000 1) g. The first mass was obtained as the difference between the masses of the ampoule before and after the transfer. The second was calculated from its activity: the ampoule plus residue was filled with distilled water to the same level as was the case, originally, for the active solution, and counting was carried out by means of a Ge detector. The activity so determined yields the mass of the (residual) activity according to a calibration carried out earlier.

(2) About 0.4 g of original solution for dilution.

Table 3 – Results of ionization-chamber measurements of activity and adsorption tests for remaining activity

Laboratory	Activity concentration at reference date ($kBq\ g^{-1}$)			Activity remaining in the "empty" ampoule after 2 rinsings with distilled water (Bq)		Measuring instrument used for adsorption tests	Number of additional rinsings		Final residual activity (Bq)	
AECL				92 ± 12		Ge detector			92	
CNEN				110		HP Ge detector			110	
ENEA				96	1	NaI well type detector	1		27	
ETL				501	2	Ortec GMX 20190 Ge γ-ray spectrometer				
IEA	1 413	t		25 ± 5	3	single NaI(Tl) detector				
LMRI	1 436	o	4							
NAC				89	5	NaI detector	3		36	
NIM	1 531	t	6	100	6	4πLS	3		100	
NIST				43	7	127x127 mm NaI(Tl) well detector				
NPL	1 420.9	t	8			NPL "671" type ionization chamber	1	9	100	10
NRC	1 419 ± 7	o	11	660	11	Ge-Li				
	1 417 ± 7	t	12							
OMH	1 441	o	13	530 ± 30	15	calibrated γ spectrometer (HP Ge detector with a Be window)	2 with diluent		30 ± 10	15
	1 439	t	14							
PSPKR	5 205.8	o	16	0	16	ionization chamber	2		0	
	5 497.2	t	16							
PTB	1 425 ± 5	o	17			calibrated ionization chamber	19			
	1 425 ± 2	t	18							

Table 3 (continued)

o	before opening	
t	after transfer	
1	date of the test	1988-06-28
2	date of the test	1988-06-10
3	date of the test	1988-06-14
4	date of the measurement	1988-04-27
5	date of the test	1988-05-16
6	date of the test	1988-05-14
7	date of the test	1988-05-09
8	date of the measurement	1988-05-26
9	rinsing with carrier	
10	date of the test	1988-06-22
11	date of the measurement	1988-05-10
12	date of the measurement	1988-05-12
13	date of the measurement	1988-05-11
14	date of the measurement	1988-05-18 and 1988-06-16
15	date of the test	1988-05-12
16	date of the measurement	1988-06-20
17	date of the measurement	1988-04-27 and 1988-04-28
18	date of the measurement	1988-05-04 to 1988-06-15
19	calibrated using the PTB value from trial comparison 1987 [2]	

Table 4 - Source preparation for electron counting

Laboratory and method*	Diluent	Nb. of dil.	Dilution factor	Source backing: Substrate metal coating	Source backing: Number of films	Source backing: Number of metal layers	Total mass ($\mu g\ cm^{-2}$)	Wetting or seeding agent	Drying	Spec. treatment	Range of source mass (mg)	Nb. of sources used	Type of balance used
AECL** 3	0.001 M NaOH + 25 mg/l NaI + 60 mg/l Na_2SO_3	2	16.667 40.280	VYNS Au-Pd	1	0 a 1 b	15 - 20	Catanac SN [1]	normal lab. air without heating	2	0.25 to 1.04 [3] 10 to 42 [4]	6	Mettler M5
CBNM 4	5×10^{-4} mol/l NaOH + 2×10^{-4} mol/l NaI + 10^{-4} mol/l $Na_2S_2O_3$	3	12.072 7 25.148 4 42.213 6	VYNS	1				[5]	6	8 to 32	8	Mettler M5
ETL 3	5×10^{-4} mol/l NaOH + 50 µg KI + 50 µg $Na_2S_2O_3$	2	9.430 75 7.754 19	VYNS [7] Au [8]	1	0 a 2 b	5 [9]		simple drying in a silical gel dessicator	10	9.8 to 20.3	8	Mettler M5
NPL 3	5×10^{-4} mol/l NaOH + 50 µg/g sol. I/KI + 50 µg/g sol. $Na_2S_2O_3$	1	3.004 36 [11]	VYNS Au	1	1 a 1 b	30	Catanac at 50 µg/g	in air at ambient temperature	12	12 to 26	10	Mettler M5
NRC 3			MS	VYNS Au-Pd	1	0 a 2 b	25	Catanac SN	warm air	13	10 to 23	8	Mettler M5
VNIIM 3	0.02 g/l $NaHCo_3$ + 0.05 g/l KI + 0.05 g/l Na_2SO_3	2	4.933 5.796	X-ray film Au	1	1 a 1 b	40	Insulin	ambient atmosph.	14	20 to 40	7	CMO-1000

Table 4 (continued)

* The figures in this column refer to the methods used, as listed in paragraph 8 of the Table of contents.

** Used also for method 2.

a Above.
b Below.

[1] On some sources.

[2] - Two sources by dispensing solution into 10 µl of 240 mg/l $AgNO_3$ of aqueous solution,
- Four sources by dispensing solution into 15 µl of 240 mg/l $AgNO_3$ of aqueous solution.

[3] Of original solution.

[4] Of a dilution.

[5] Half an hour under humid atmosphere to allow for reaction, then dried in ambient air.

[6] An aliquot of $AgNO_3$ was added twice.

[7] 15 µg cm^{-2}.

[8] 15 µg cm^{-2} + 15 µg cm^{-2}.

[9] Mean superficial density of solid contents of diluted solution including Ag.

[10] One drop of a freshly prepared 0.01 mg/g $AgNO_3$ of solution was added just after dispensing the radioactive solution onto source mount.

[11] Dilution factor determined by weighting but checked by means of an ionization chamber with ampoules which agreed to about 0.5 %.

[12] For each drop of iodine solution deposited on VYNS the laboratory added:
- one drop $AgNO_3$ nitrate at 100 µg/g
- one drop Catanac at 50 µg/g
- one drop 0.01 M NaOH.

[13] Precipitated with $AgNO_3$.

[14] One drop of $AgNO_3$ (75 µg/g of solution) was deposited on the active solution.

Table 5 - Source preparation for X- and/or γ-ray counting

Laboratory and method*	Diluent per 1 or g of solution	Nb. of dil.	Dilution factor	Substrate	Number of films	Total mass ($\mu g\ cm^{-2}$)	Wetting or seeding agent	Drying	Special treatment	Range of source mass (mg)	Nb. of sources used	Type of balance used	Remarks
AECL 1, 2	10^{-3} mol/1 NaOH + 25 mg/1 NaI + 60 mg/1 Na_2SO_3	2	16.667 40.280	polyester tape	2 sandw.	6 300		normal lab. air no heating	1	0.25 to 2.4 [2] 10 to 40 [3]	6	Mettler M5	
BIPM 1, 2	$5 \cdot 10^{-4}$ mol/1 NaOH + 50 μg/g KI + 50 μg/g $Na_2S_2O_3$	1	40.470 7	VYNS	2	30		in air at ambient temperature	4	12 to 55		Mettler M5 [5] Sartorius UM [6]	
CBNM 1, 2	$5 \cdot 10^{-4}$ mol/1 NaOH + $2 \cdot 10^{-4}$ mol/1 NaI + 10^{-4} mol/1 $Na_2S_2O_3$	3	12.072 7 25.148 4 42.213 6	VYNS	1	6 700		[7]	added 2x aliquot $AgNO_3$	8 to 32	8	Mettler M5	
CNEN 1, 2, 4	$5 \cdot 10^{-4}$ mol/1 NaOH + 50 μg/g KI + 50 μg/g $Na_2S_2O_3$	3	7.821 2 5.902 5 9.352 8	collodion [1 2] VYNS [4]	1 [1 2] 2 [4]	20		dry air	[8]	8 to 50	20	Mettler M5 SA	[9]
ENEA 1	$5 \cdot 10^{-4}$ mol/1 NaOH + 50 μg/g I/KI + 50 μg $Na_2S_2O_3$	2	15.077 9 ± 0.001 2 51.917 6 ± 0.004 6							13 to 105 26 to 151	25	Mettler M5	[10]
ETL 1	$5 \cdot 10^{-4}$ mol/1 NaOH + 50 μg KI + 50 μg $Na_2S_2O_3$	2	9.430 75 7.754 19	VYNS [11]		2 000		simple drying in a silica-gel dessicator	[12]	11.5 to 18.9	14 [13]	Mettler M5	
IEA 2			MS	mylar tape 0.4 mg cm^{-2}	1	40		air	[14]	3.8 to 10.1	13	Mettler UM3/36	

Table 5 (continued)

Laboratory and method*	Diluent per 1 or g of solution	Nb. of dil.	Dilution factor	Substrate	Number of films	Total mass ($\mu g\ cm^{-2}$)	Wetting or seeding agent	Drying	Special treatment	Range of source mass (mg)	Nb. of sources used	Type of balance used	Remarks
KSRI 4			MS	collodion	2	30 to 40	15	air	16	12 to 24	7	Mettler M5 SA	
LMRI 2	$5 \cdot 10^{-4}$ mol/l NaOH + 50 µg/g I/KI + 50 µg/g $Na_2S_2O_3$	1	41.750 1 ± 0.001 2	mylar	2	40		dried air under infra red lamp		8 to 31	7	Mettler M5	
NAC 1			MS	plastic tape	1 sandw.			infrared lamp at 50 cm dist.		1.96 to 44.9	8	Mettler M3	dry sources
	108 mg/l NaI +174 mg/l $Na_2S_2O_3,5H_2O$	1	2.045	17						4.5 to 38.8	8	Mettler M3	liquid "
2, 4			MS	plastic tape	1 sandw.			infrared lamp		36.76 to 49.54	7	Mettler M3	18
NIM 2	20 µg/l NaOH + 50 µg/ml I/NaI + 133 µg/ml $Na_2S_2O_3$	1	1.131 8	mylar (3.5 mg cm^{-2}) Al (8.3 mg cm^{-2})	2 mylar 2 Al	11 800x2		air	19	10 to 17	10	TG 332A	20
NIST 1	0.26 to 0.75 µg/g NaOH + 56 µg/g KI + 215 µg/g LiOH + 0.65 to 1.81 µg/g $Na_2S_2O_3$	3	26.722 4 32.817 4 76.774 5	ion exchange paper strips (L = 20 mm w = 4 mm t = 0.3 mm)	2 myl. films 0.006 cm thick	6 000 to 13 000		room air	20	15.787 to 34.593	10	Mettler M5	21
1 bis	56.14 µg/g KI + 221.6 µg/g LiOH + 27.59 µg/g Na_2SO_3 [22]	3	26.722 418 32.817 379 76.774 527	anion [23] exchange paper disks	[24]	15 000 to 30 000		dried air at room temperature		8.263 to 89.643	33	Mettler M5	25

Table 5 (continued)

Laboratory and method*	Diluent per 1 or g of solution	Nb. of dil.	Dilution factor	Substrate	Number of films	Total mass ($\mu g\ cm^{-2}$)	Wetting or seeding agent	Drying	Special treatment	Range of source mass (mg)	Nb. of sources used	Type of balance used	Remarks
NRC 5, 6			MS	VYNS coated with Au-Pd	1	0 above 2 below 25	catanac SN	warm air	26	10 to 23	8 27	Mettler microgramatic M5	
OMH 1	10^{-3} mol/1 NaOH + 50 µg/g I/KI + 50 µg/g KIO_3 + 50 µg/g $Na_2S_2O_3$	1	19.441 ± 0.002							12 to 87		Mettler M5 SA	28
PSPKR 2, 4	0.02 g/1 LiOH + 0.05 g/1 KI + 0.02 g/1 Na_2SO_3 in H_2O	1	5.263	mylar	2			29		5.27 to 26.06	6	Mettler semi-micro	
PTB 1	60 µg/g NaI + 45 µg/g $Na_2S_2O_3$	2	5.4 7.8	VYNS coated with Au-Pd	1 or 2	50		air	26	6 to 10	15	Mettler ME22 micro	
4			MS	VYNS coated with Au-Pd	1 or 2	50		air	26	6 to 10	7	Mettler ME22 micro	30
UVVVR 1, 2	50 µg/g KI 31 + 50 µg/g $Na_2S_2O_3$	2	10.603 3 10.923 5	polyethylene	2 sandw.	4 700	insulin		ludox	20 to 40	10	Sartorius 1801	
VNIIM 2			MS	X-ray film	2	200		ambient atmosphere	27	50 to 100	7 32	CMD-1000	

Table 5 (continued)

* The figures in this column refer to the methods used, as listed in paragraph 8 of the Table of contents.

MS Master solution.

1 Three sources were produced by dispensing solutions into 10 µl of 240 mg/l $AgNO_3$ aqueous solution and three by dispensing the solution into 15 µl of 240 mg/l $AgNO_3$ aqueous solution.

2 Of the original solution.

3 Of a dilution.

4 Addition of one drop of a 200 µg/g HNO_3 solution to each source.

5 For dilution.

6 For sources.

7 Half an hour under humid atmosphere to allow for reaction, then dried in ambient air.

8 A drop of a 160 µg/g $AgNO_3$ solution was deposited on the active solution.

9 After drying the deposit was covered with a layer of VYNS.

10 The sources used were glass ampoules treated with a hydrophobic agent; drops of diluted solutions were put in the ampoules which were filled to 1 cm^3 with diluent solution and flame sealed;
diameter of the body of ampoules: 17 mm,
height of liquid in the ampoules: 5 mm.

11 The foils were sealed in polyethylene sheets after drying.

12 One drop of a freshly prepared aqueous solution containing 0.1 mg/g $AgNO_3$ was added.

13 For method 3 only 8 sources were measured in 16 different conditions.

14 The active solution was deposited on a drop of double excess of $AgNO_3$ solution.

15 A drop of ludox SM $15 \cdot 10^{-4}$ solution was deposited on the active solution.

16 A drop of $AgNO_3$ solution diluted by a factor 10 was deposited on the active solution (≈ 15 mg of solution).

Table 5 (continued)

17 The dilution was used to prepare liquid sources which were placed in glass counting vials (2.5 cm in diameter) where 1 ml of distilled water was poured.

18 The balance was found to be slightly unstable, leading to larger weighing uncertainties than usual.

19 A drop of solution of $AgNO_3$ (1 mg/ml) was deposited on the active solution.

20 Ion exchange resin was used.

21 Measurements performed by C. Ballaux.

22 Per gram of carrier.

23 Diameters from 6 mm to 22 mm.

24 Two layers of polyester tape 0.006 cm thick.

25 Measurements performed by Dan Golas and Don Gray.

26 Precipitated with $AgNO_3$.

27 A drop of $AgNO_3$ (22 μg/g of solution) was deposited on the active solution.

28 The active solution was put in brown medical glass ampoules with a body diameter of 15 mm; the height of liquid was 8 mm; all ampoules were filled to 1 g.

29 At room temperature (dessicator with silica gel).

30 Three groups of 5 sources each were produced, each group after transfer of the solution to a PTB ampoule and ionization chamber measurement.

31 Per gram of water.

32 Nine sources were measured with method 3.

Table 6 - Liquid-scintillation counting

Laboratory and method*	Counting vessel	Nb. of dilut.	Dilution factor	Diluent	Number of sources used	Composition of the scintillation solution	Remarks
NAC 6	glass 20 ml	1	2.045	108 mg/l NaI + 174 mg/l $Na_2S_2O_3,5H_2O$	7	12 ml of a commercial xylene-based scintillation cocktail (Instagel from Packard)	each source comprised about 45 mg of dilution

* The figure in this column refers to the method used, as listed in paragraph 8 of the Table of contents.

Table 7 – 4π proportional counters used by the participants

Laboratory and method*	Wall material	Height of each half (mm)	Anode: Material	Anode: Diameter (mm)	Anode: Length (mm)	Anode: Distance from source (mm)	Anode: Voltage applied (kV)	Gas	Pressure (MPa)	Discrimination level (keV)	Dead time (μs)
AECL [3]	stainless steel [1]	21	W (Au coated)	0.013	36	10	1.8 to 2.5 [2]	CH_4	0.1	0.1 to 5 [3]	2.55 ± 0.03
ETL [4]	brass Au coated [4, 5]	20	W (Au coated)	0.05	70	10	2.4/2.5	Ar + 10 % CH_4	0.1	0.5 to 2	7.85
NPL [4]	Cu and perspex (Ag coated) [6]	14	Mo (Au coated)	0.075	75	8	1.875 to 2.3	Ar–CH_4	0.1	0.3 [7]	1.48
NRC [4, 7, 8]	Al	25.4	stainless steel	0.025	38	12.7	1.5	Ar–CH_4 CH_4	0.1	60 to 460 (mV)	2.1
VNIIM [4]	Al [8]	20	W	0.03	100	15	2 to 3.2	Ar + 10 % CH_4	0.1	0.3	2.0 ± 0.1

* The figures in this column refer to the methods used, as listed in paragraph 8 of the Table of contents.

[1] The upper and lower walls of the proportional counter opposite to the source and facing the NaI(Tl) detectors consisted of 0.9 mg cm^{-2} Al-coated polyester film. A schematic view of the detector is given in [4].

[2] The voltage was varied to produce an effective change in the discrimination level.

[3] At low electron energies the detection efficiency is varied by changing the bias voltage applied to the 4π proportional counter to vary the gas amplification [5].

[4] The proportional counter had the shape of a rectangular box.

[5] The top of the counter was replaced by an Al foil 0.2 mm thick.

[6] The top of one half of the proportional counter contained a large window of mylar, coated on both sides with Al (total density 0.9 mg cm^{-2}) to enable X rays to reach the Ge detector (Fig. 2).

[7] This value was chosen in the centre of the plateau.

[8] The proportional counter was pill-box shaped.

Table 8 - Scintillation detectors for X- and γ-ray detection, dead times

Laboratory and method*	Number and nature of crystals		Scintillation detectors				Phototube	Resolution		Solid angle	Distance counter-source	Dead times for γ- and/or X-ray channel
	ordinary	well type	outer dim. diam. (mm)	outer dim. height (mm)	hole size diam. (mm)	hole size depth (mm)		(FWHM**) (%)	(keV)	(sr/4π)	(mm)	(μs)
AECL 1												[1]
2,3	2 NaI(Tl)		51	1				34 (at 28 keV)	9.5	0.43	4	2.55 ± 0.03
BIPM 1,2	2 NaI(Tl) [2]		76.2	76.2			2 RCA8054	7 (at 662 keV) [3]	46.3	0.688	25	5.001 ± 0.004 on both channels
CBNM 1		NaI(Tl)	152.4	152.4	50	100		29 (at 27.5 keV)	8	0.983	10 to 20	[4]
2,3	2 NaI(Tl)		51	6				33 (at 27 keV)	9	0.08 to 0.796	1 to 50	5.9
5		2 CsI(Tl) [5]	51	24	10	5		25 (at 60 keV)	15	~ 1	0.0035 [6]	10.6
CNEN 1,2	2 NaI(Tl)		76	76				22.2 (at 28 keV) [7]	6.2		10	3.100 ± 0.040 3.172 ± 0.038
4	2 NaI(Tl)		51	6				57 (at 28 keV)	16	0.015 to 0.485	1 to 100	5.20 ± 0.05 on both channels
ENEA 1		NaI(Tl)	82	104	25	70.5		24 (at 28 keV)	6.7	0.991	4	5.00 ± 0.02
ETL 1		NaI(Tl)	50.8	50.8	17	34		26 (at 28 keV)	7.3	0.75	0	[8]
3	NaI(Tl)		37.6	2				40 (at 28 keV)	11		30	2.5
IEA 2	2 NaI(Tl)		25	5				8 (at 662 keV)	53	0.028	6.5	8

Table 8 (continued)

Laboratory and method*	Number and nature of crystals: ordinary	Number and nature of crystals: well type	Scintillation detectors: outer dim. diam. (mm)	Scintillation detectors: outer dim. height (mm)	Scintillation detectors: hole size diam. (mm)	Scintillation detectors: hole size depth (mm)	Phototube	Resolution (FWHM**) (%)	Resolution (keV)	Solid angle (sr/4π)	Distance counter-source (mm)	Dead times for γ- and/or X-ray channel (μs)
KSRI 4	2 NaI(Tl)		38.1	1				16.8 (at 59.5 keV)	10		1 to 150	4.00
LMRI 2	2 NaI(Tl)		44	2							~ 25	20
NAC 1	NaI(Tl)		75	75				9.5 (at 662 keV)	63	⩽ 0.5	0	1.22
2,4	2 NaI(Tl)		50	50				7.0 (at 662 keV)	46	⩽ 0.5	3 to 100	3.192
6	NaI(Tl)		75	75			2 RCA8850[9]					54.0
NIM 2	2 NaI(Tl)	[10]	40	2				30 (at 59.6 keV) [11]	18		~ 15	4.2
NIST 1		NaI(Tl)	50.8	50.8	6.7	50.8 [12]		27 (at 28 keV) [13]	7.6	0.987	4 [14]	[15]
1bis	2 NaI(Tl)[16]		24.6	[17]				25 (at 28 keV) [18]	7	0.8	~ 2.5	[15]
NPL 4												19.9
NRC 3	2 NaI(Tl)		76	76				7 (at 662 keV)	46		33	2.01 ± 0.002 [19] 5.06 [20]
7,8	2 NaI(Tl)		50.8	1.0				50 (at 5.9 keV)	3		33	2.10 ± 0.02
OMH 1		NaI(Tl)	28	35	16	29		19.2 (at 59.5 keV)	11.4	0.975		
PSPKR 1		NaI(Tl)	115	90	20	65		27 (at 28 keV)	7.6		5	
2	2 NaI(Tl)		176	76				19 (at 28 keV)	5.3		1.8	5.0
4	2 NaI(Tl)		176	76				19 (at 28 keV)	5.3		0.3 to 4.3	5.0

Table 8 (continued)

Laboratory and method*	Number and nature of crystals		Scintillation detectors				Phototube	Resolution		Solid angle	Distance counter-source (mm)	Dead times for γ- and/or X-ray channel (μs)
	ordinary	well type	outer dim. diam. (mm)	outer dim. height (mm)	hole size diam. (mm)	hole size depth (mm)		(FWHM**) (%)	(keV)	(sr/4π)		
PTB 1	21											
4	2 NaI(Tl)		75	6				~ 30 (at 30 keV)		⩽ 0.5	3 to 150	5.00 ± 0.05
UVVVR	2 NaI(Tl)		40	20				30 (at 28 keV)	8.4	22	0.05	
VNIIM 2,3	2 NaI(Tl)[10]	10	40	3				23 (at 28 keV)	6.5	0.01	8 to 12	1.5 ± 0.1

Table 8 (continued)

* The figures in this column refer to the methods used, as listed in paragraph 8 of the Table of contents.

** FWHM = full width at half maximum

1 Live-time measurements.

2 Only one for method 1; in this case the solid angle was 0.344 ($sr/4\pi$).

3 For one detector; for the other one the resolution was 6.7 % (44.5 keV) at 662 keV.

4 Live-time correction of the multichannel analyzer Canberra S100.

5 For further details on the detector system, see [6].

6 Foil thickness.

7 For one detector; for the other one the resolution was 24.8 % (6.9 keV) at 28 keV.

8 Live-time mode was used.

9 These phototubes were used to detect electrons.

10 With a Be window.

11 For one detector; for the other one the resolution was 26 % (16 keV) at 59.6 keV.

12 Through hole.

13 At 59.4 keV the resolution of the detector was 18 % (10.7 keV).

14 Mean distance between photon counter and source center.

15 Live-time correction of the multichannel analyzer.

16 Two independent measurements were made using the same method.

17 One detector was 0.4 mm high, the other 0.8 mm high.

18 At 59 keV the resolution of the detector was 15 % (9 keV).

19 Fixed dead time for the gamma monitor channels.

20 Common extending dead time for the β and anticoincidence γ channels.

21 The sum-peak activity measurements were based on method 1 modified for peak area evaluations with a highly-resolving Si(Li) detector.

22 1 for method 1 and 2•0.5 for method 2.

Table 9 - Semi-conductor detectors for X- and γ-ray detection, dead times

Laboratory and method*	Semi-conductor detector: Nature and type	Dimensions ϕ (mm) h (mm)	Volume (cm^3)	Relative efficiency (%)	Energy resolution FWHM** (keV)	Window: material	Window: thickness (mm)	Solid angle (sr/4π)	Distance between counter and source (mm)	Dead times for γ- and/or X-ray channel (μs)
AECL 1	Ge	440, 35		3.4 at 28 keV	0.93 at 28 keV	Be	0.13	0.083	35	2.55 ± 0.03 [1]
NPL 3	Ge-N type		85		0.92 at 122 keV	Al	1.0		40 [2]	19.9
NRC 3	2 Ge(Li)				2.2 at 662 keV				40	2.01 ± 0.002 [3] 5.06 [4]
NRC 7, 8	Si(Li)	6, 6			0.170 at 5.9 keV	Be	0.13		45	2.10 ± 0.02
PTB 1	Si(Li) [5]	16, 5			3.6 at 5.9 keV	Be	0.05		8.5	

* The figures in this column refer to the methods used, as listed in paragraph 8 of the Table of contents.
** FWHM = full width at half maximum.

1 Live-time measurements.
2 Distance between face of Ge crystal and source = 45 mm.
3 Fixed dead time for the gamma monitor channels.
4 Common extending dead time for the beta and anti-coincidence gamma channels.
5 The sum-peak activity measurements were based on method 1 modified for peak-area evaluations with a highly-resolving Si(Li) detector.

Table 10

Coincidence and anticoincidence counting

Laboratory & method*	Dead times τ_e (μs)	Dead times τ_γ (μs)	Coincidence resolving times	Remarks
AECL 2,3	2.55 ± 0.03	2.55 ± 0.03 [1]	0.72 ± 0.01	[2]
BIPM 1		5.001 ± 0.004 [1]	0.239 ± 0.001	
CBNM 2,4		5.90 ± 0.02 [1]	0.80 ± 0.08	Dead times determined with the two-pulser method.
CNEN 1,2		3.100 ± 0.040 [3] 3.172 ± 0.038 [4] 5.20 ± 0.05 [1]	0.952 9 ± 0.000 9 [3] 0.980 6 ± 0.001 0 [4] 0.802 ± 0.004 [1]	Accidental coincidence rate observed with uncorrelated random pulses.
ENEA 1		5.00 ± 0.02		
ETL 3	7.85 ± 0.10	2.5 ± 0.1	0.815 ± 0.05	Dead times determined by the double-pulse generator method and coincidence resolving time determined by the source-pulser method.
IEA 2		8 ± 0.2 [1]	1 ± 0.05	Dead times and coincidence resolving times determined by means of two oscillators.
KSRI 4		4.00 ± 0.01 [1]	1.05 ± 0.005	Dead times and coincidence resolving time determined by means of a calibrated oscilloscope (Tektronix 2465).
LMRI		20 [1]	0.500	
NAC 1 2,4 6	 from 1.005 to 1.135 [5 7]	1.22 3.192 ± 0.036 [1 5] 54.0 ± 1.0 [5]	 0.495 0 ± 0.001 4 [6] 0.47 ± 0.004 [6]	
NIM		4.2 ± 0.2 [1]	0.98 ± 0.05 [2]	The coincidence resolving time was determined using accidental coincidences.
NPL	1.48 ± 0.02	19.9 ± 0.1	0.70 ± 0.02 [2]	Dead times were determined by means of a tail-pulse generator with a calibrated oscilloscope.
IMM 2 4	 2.0 ± 0.1	1.5 ± 0.1 [1] 2.0 ± 0.1	0.5 ± 0.02 2.0 ± 0.1	Dead times determined by means of a source and a generator. Coincidence resolving time obtained using the delayed coincidence curve.
NRC 3	2.10 ± 0.02 [2]	live time corrections	0.950 ± 0.050 [2]	
7	2.01 ± 0.002 [8]	5.06 ± 0.05 [9]		

Table 10 (continued)

Laboratory & method*	Dead times τ_e (μs)	Dead times τ_γ (μs)	Coincidence resolving times (μs)	Remarks
OMH		6.045 ± 0.005 [10]		
PSPKR 1		5.0 [1]	1.0	Fixed dead times.
PTB 2,4		5.00 ± 0.05 [1]	1.00 ± 0.02	Dead times and coincidence resolving time have been determined by the two-oscillator method.
UVVVR 4		5.987 ± 0.010 [11]	0.498 ± 0.006 [2]	Dead times have been determined by means of the two-oscillator method.
VNIIM 2		1.5 ± 0.1 [1]	0.5 ± 0.02	Dead times determined by means of a source and a generator. Coincidence resolving time obtained using the delayed coincidence curve.
4	2.0 ± 0.1	2.0 ± 0.1	2.0 ± 0.1	

* The figures in this column refer to the methods used, as listed in paragraph 8 of the Table of contents.

[1] On both channels.

[2] Dead times determined by the source-pulser method as described in [7].

[3] Values for the first window (16 keV to 45 keV) on both detectors and for both methods.

[4] Values for the second window for both detectors: method 1 (45 keV to 72 keV), method 2 (16 keV to 72 keV).

[5] The outputs from NaI(Tl) detectors and preamplifiers were terminated into a 50 Ω power divider at the input of the amplifier. No change in geometry and detectors was made. Only the high-voltage supply to each detector was alternatively switched on and off.

$\tau_D = \frac{t}{m_{12}} \{1 - [1 - \frac{m_{12}(m_1+m_2-m_{12})}{m_1 m_2}]^{1/2}\}$, where m_1 and m_2 are the counts obtained from the separate channels, m_{12} the combined count and t the counting time.

[6] Each NaI(Tl) detector viewed an independent ^{125}I source. The discriminator outputs from each X-ray channel were fed to the inputs of the coincidence unit. The resolving time was calculated from $\tau_R = ct/2m_1m_2$, where m_1 and m_2 are the counts obtained from the separate channels, c the random coincidence count and t the counting time.

[7] The value of the dead time in the electron channel depends on the bias setting.

[8] For gamma monitor channels.

[9] For beta and anticoincidence gamma channels common extending dead time.

[10] For one channel; for the other τ_2 = (6.035 ± 0.005) μs.

[11] For one channel; for the other τ_2 = (5.985 ± 0.010) μs.

Table 11 - Counting data for the different methods

Laboratory and method*	Window limits or discrim.threshold (keV)	Typical count rates (s^{-1})	Background rates (s^{-1})	Number of sources measured	Typical time for one measurement (s)	Date of measurement
AECL 1						88-07-14
2	10 to 90	100 to 1 700	0.3 ± 0.1	6	1 000	88-07-11 to 88-08-29
3	0.1 to 5	250 to 1 250	0.5 ± 0.5	6	1 000	88-07-20 to 88-08-13
BIPM 1,2		80 to 270	2.2	24	10 800 [1]	88-06-06 to 88-06-29
CBNM 1	0 to 86	1 500	16	6	15 000	around 88-05-15 [2]
2	7 to 20 [3] end of amplif. [4]	50 to 1 000	4	4	1 000 [5]	"
4	7 to 20 [3] end of amplif. [4]	50 to 1 000	4	4	1 000 [5]	"
5	7.4 [6]	300 to 1 800	4.1	8	20 000	"
CNEN 1	16 to 45 [7] 45 to 72 [8]	400 to 2 500	5.7	20	5 400	88-06-09 to 88-06-30
2	16 to 45 16 to 72	400 to 2 500	5.7	20	5 400	"
4	10 to 100	3 000	20	9	200 to 10 000	88-06-01 to 88-06-30
ENEA 1	10 to 40 [7] 40 to 80 [8]	2 000 [7] 600 [8]	1.75 [7] 0.75 [8]	25	600	88-05-06 to 88-06-23
ETL 1	14 to 43 [7] 43 to 82 [8]	1 000 [7] 600 [8]	1.36 [7] 0.76 [8]	14	2 000	88-06-26
3 [9]	10 to 43	130	0.6	8 [11]	1 500	88-06-30
	0.5 to 3	800 [10]	6	8 [11]	1 500	
IEA 2	60 [12]	3 000	1.8	13	1 800	88-06-15
KSRI 4	14 to 76	200 to 6 000	8	7	600	88-07-04
LMRI 2		500	5	7	2 000	88-05-05 to 88-06-29
NAC 1	14 to 42 [12]	900 to 21 000	1.9	8	200 to 1 000	88-06-15 to 88-06-16
2,4	22.5	12 275 [13] 730 [14]	9 [15]	7	400 [13] 8 000 [14]	88-06-13 to 88-06-16
6	45 to 70 [12 16 17]	34	1.06	7	3 000	88-06-14
	⩾ 2 [18]	26 000	6 to 20	7	3 000	
NIM 1	14	1 500	3 to 8	10	1 200	88-08-17 to 88-08-18
NIST 1	[19]	1 000 [20]	1.33	10	2x3 000	88-05-10 to 88-05-15
1bis	2 to 100	150 to 2 000	0.3	33	4 000	88-06-17

Table 11 (continued)

Laboratory and method*	Window limits or discrim.threshold (keV)	Typical count rates (s^{-1})	Background rates (s^{-1})	Number of sources measured	Typical time for one measurement (s)	Date of measurement
NPL 3 [21]	25.6 to 33.5	300	0.15	10	500	88-06-23
22	0.3	3 000	2	10	500	"
NRC 7 [22]	60 to 460 [23]	12 000 to 35 000 [24]	0.5	8	10 800	88-05-15
8 [22]	60 to 460 [23]	12 000 to 35 000 [25]	0.5	8	10 800	"
OMH 1	13 to 43 [7]	3 000 [26]	0.3	18	1 000	88-05-17 to 88-05-20
	43 to 78 [8]					88-06-14 to 88-06-17
PSPKR 1		200 to 2 300	7.1 [7]	9	1 000	88-07-05 to 88-07-06
			43 [8]			
2	15 to 44	870 to 1 500	3.0	6	160	88-07-05 to 88-07-14
4	15 to 44	870 to 1 500	3.0	6	800	" "
PTB 1	20 to 38 [7]	400	0.04	7 [27]	10 000	88-06-25
	38 to 69 [8]					
4	17 to 100	20 000 [28]	2	15	1 000 [29]	88-05-03 to 88-06-28
UVVVR 1	12 to 41 [7]	2 880	3.3	10	10x100	88-05-19 to 88-05-24
	41 to 128 [8]					
2	12 to 128	2 880	3.3	10	10x100	"
VNIIM 2	20 to 40 [12]	2 300 [30]	0.2	7	2 000	88-05-18
		3 000 to 6 000 [31]	2 to 5	9	2 000	88-05-18
3		600 [32]	2			
		130 to 400 [31] [33]	0.05			"

Table 11 (continued)

* The figures in this column refer to the methods used, as listed in paragraph 8 of the Table of contents.

1 From one source of very low activity: 86 400 s; for the other sources: 7 200 s.

2 The measurements have been repeated around 1988-06-15.

3 Low-level discriminator.

4 Upper level discriminator.

5 For one data point. 255 data points were measured.

6 Extrapolation.

7 For the single peak.

8 For the sum peak.

9 Counting data for X and γ rays.

10 Counting data for electrons.

11 Under 16 different conditions.

12 Discrimination window.

13 At 3 mm.

14 At 100 mm.

15 The coincidence background rate varied with distance and was 0.185 s^{-1} at 3 mm and 0.012 s^{-1} at 100 mm.

16 Counting data for X and γ rays.

17 Sum peak only.

18 Counting data for electrons.

19 Extrapolated to zero energy.

20 Spectrum measured between 6 and 110 keV to include triple (accidental) coincidences.

21 X- and γ-ray counting.

22 Electron counting.

23 In mV.

24 82 measurements were made.

25 36 measurements were made.

26 For the total spectrum.

27 27 measurements were performed.

28 At low source-detector distances.

29 Time for one data point. One extrapolation needed about 50 to 400 data points. Maximum value at low distance.

30 4π proportional counter.

31 For ε_{min} and ε_{max}, respectively, where $\varepsilon = N_c/N_\gamma$ varies between 0.15 and 0.65.

32 Scintillation counter.

33 For the coincidence channel.

Table 12 - Corrections applied in calculating results

Laboratory	Method *	Background (%)	Decay (%)	Tailing of peak (%)	Decay scheme data	Dead time (%)	Remarks
AECL	2						The X-X coincidence rates were corrected for accidental coincidences.
	3						Individual e-X coincidence rates were corrected for delay mismatch and accidental coincidences.
BIPM	1, 2				$P_K = 0.797 \pm 0.001$ $\omega_K = 0.877 \pm 0.020$ $P_\gamma = 0.066\ 7 \pm 0.001\ 3$ $\alpha_K = 11.9 \pm 0.2$ $\alpha = 14.0 \pm 0.3$ [1]		$P_\gamma = 1/(1 + \alpha)$. $P_1 = P_K\omega_K$; $P_2 = (1 + \alpha_K\omega_K)/(1 + \alpha)$. $(P_1P_2)/(P_1 + P_2)^2 = 0.249\ 5 \pm 0.000\ 8$. $K = P_\gamma(1 + \alpha_K\omega_K)/P_K\omega_K$.
CBNM	1	1	12	0.5	$P_K = 0.796\ 9 \pm 0.001\ 7$ $\omega_K = 0.875 \pm 0.011$ $P_\gamma = 0.066\ 7 \pm 0.002\ 2$ $\alpha_K = 11.9 \pm 0.5$		
	2, 4	0.4	12		$K' = 0.998\ 1 \pm 0.002\ 2$ [2]	0.6	The Cox-Isham formulae [14] for dead-time corrections were used.
	5	0.2 to 1.4		0.2 to 0.4 [3]	$\alpha_{L+} = 2.09$	0.3 to 1.8	Other corrections applied: - solid angle 0.04 %, - self-absorption for electrons 3 %, - foil absorption for electrons 0.48 %.
CNEN	1				[4]		Extrapolation to zero count rate.
	2				[4]		The Cox-Isham formulae [14] were used for correcting the count rates.
ENEA	1						$(P_1P_2)/(P_1 + P_2)^2 = 0.249\ 4 \pm 0.000\ 5$. The peak separation was done by a linear extrapolation on tails. The accidental summing in the coincidence peak was taken into account by an extrapolation to zero count rate.

Table 12 (continued)

Laboratory	Method *	Background (%)	Decay (%)	Tailing of peak (%)	Decay scheme data	Dead time (%)	Remarks
ETL	1				$P_K = 0.796\ 9$ $\omega_K = 0.877$ $\alpha_K = 11.986$ $\alpha = 14.02$		Effect due to the accidental sum in the pulse-height distribution. The results were corrected by extrapolating back to zero source strength (see Fig. 1). $P_1 = P_K\omega_K = 0.698\ 6.$ $P_2 = (\alpha_K\omega_K + 1)/(1 + \alpha) = 0.766\ 4.$ $P_1P_2/(P_1 + P_2)^2 = 0.249\ 40.$ $N_o = [(N_1 + 2\ N_2)^2/N_2]\ [P_1P_2/(P_1 + P_2)^2]\ F$, where F is a correcting factor for accidental sum effect.
	3						10 % of correction for accidental coincidences. The Campion formulae were used [16].
IEA	2				$P_K = 0.797$ $\omega_K = 0.877$ $\alpha_K = 11.9$ $\alpha = 14.02$		
KSRI	4						Corrections for dead time, resolving time, decay and background.
LMRI	2				$P_K = 0.797$ $\omega_K = 0.877$ $\alpha_K = 11.9$ $\alpha = 14.0$		$4\ K/(1 + K)^2 = 0.998\ 1.$
NAC	1						$P_1 = 0.699;\ \ P_2 = 0.762\ 7.$
	2				$K = 1.090\ 8$ $4K/(1+K)^2 = 0.998\ 1$		Correction for background, dead time, resolving time, buoyancy, and decay. The coincidence count rate was corrected using the formula given by Bryant [15]. A formula was derived to estimate the uncertainty in N_o. For each source, measurements were made for a range of source-to-detector distances and combined to give a weighted mean and the corresponding uncertainty using the usual formulae.

Table 12 (continued)

Laboratory	Method *	Background (%)	Decay (%)	Tailing of peak (%)	Decay scheme data	Dead time (%)	Remarks
NAC	4				$K = 1.090\ 8$ $4K/(1+K)^2 = 0.998\ 1$		The same corrections as for method 2 were applied. A formula was derived to estimate the uncertainty for each y(x) measurement and used to weigh the values appropriately for the fitting process.
	6						Corrections were applied for background, dead time, coincidence resolving times (0.47 μs), satellite pulses (0.12 % to 0.23 %), buyoancy and decay.
NIM	2				$P_K = 0.797 \pm 0.001$ $\omega_K = 0.877 \pm 0.02$ $\alpha_K = 11.9 \pm 0.2$ $\alpha = 14.0 \pm 0.3$		$4\ K/(1 + K)^2 = 0.998\ 1.$
NIST	1						Sum-peak tail correction computed as 1.2 times the semi-logarithmic tail.
	1bis						Mean efficiency $\varepsilon = 0.819 \pm 0.006$. Extrapolation to zero count rate.
NPL	3						ε_β was varied by changing the high voltage in 25 V steps. The background was subtracted at each voltage (this did not change significantly over one week). The Cox-Isham (modified by Smith) formula [17] was applied to correct for dead time and resolving time.
NRC	7						The usual decay correction was made. Corrections for background and radioactive decay were applied.
	8						Corrections for background, dead time, resolving time and radioactive decay were applied.

Table 12 (continued)

Laboratory	Method *	Background (%)	Decay (%)	Tailing of peak (%)	Decay scheme data	Dead time (%)	Remarks
OMH	1				$P_1P_2/(P_1+P_2)^2$ = 0.249 4 ± 0.000 5		The count rates for the singles events N_1 and for the sum-coincidence peak events N have been corrected for dead time, background and decay. A tail correction has also been applied. An extrapolation to zero count rate has been made in order to eliminate the effect of accidental summing in N_2. Therefore, activities between 0.8 kBq and 9 kBq were measured. To obtain the area under the singles peak N_1 and the sum peak N_2, two timing single-channel units were used [5]. The singles-peak tail and the sum-peak tail have been determined graphically. $P_1 = P_K\omega_K$, $P_2 = (1+\alpha_K\omega_K)/(1+\alpha_T)$.
PSPKR	1						Extrapolation to zero count rate. Correction data for background and decay.
PTB	1				P_γ = 0.066 7		$P_1 = P_K\omega_K$ = 0.699 0; $\alpha_K\omega_K/(1+\alpha)$ = 0.695 7.
	4				K = 1.112 P_K = 0.797 ω_K = 0.877 α_K = 11.9 α = 14.0		The Cox-Isham formula [14] was used.
UVVVR	2						The Cox-Isham formula [14] was used.
VNIIM	2						$4K/(1+K)^2$ = 0.999 6.

* The figures in this column refer to the methods used, as listed in paragraph 8 of the Table of contents.

1 These values lead to K = 1.097 8 ± 0.027 6.

2 $$K' = \frac{4\,P_K\omega_K P_\gamma(\alpha_K\omega_K + 1)}{[P_K\omega_K + P_\gamma(\alpha_K\omega_K + 1)]^2}\,.$$

3 Exponential tail below 7.4 keV.

4 The same values were used as for the BIPM.

5 Canberra model 2037A combined with a dead-time generator constructed at the OMH.

Table 13 - Uncertainty components of the final result (in %)

Laboratory	A E C L			B I P M		C B N M			
Method*	1	2	3	1	2	1	2	4	5
Components due to:									
counting statistics	0.14 [1]	0.04 [3]	0.04 [9]	0.117	0.04	0.15	0.44	0.30 [12]	0.05
weighing	0.02 [4]	0.02 [4]	0.02 [4]	0.025 [5]	0.025 [5]	0.15 [10]	0.15 [10]	0.15 [10]	0.20
dead time	included	⩽ 0.01 [5]	⩽ 0.01 [5]		0.08	0.05 [11]	0.10	0.10	0.10
background	0.05 [2]	[6]	[6]	[6]	[6]	0.10	0.10	0.10	0.10
pile-up	included	⩽ 0.01				0.01			
timing	0.10	0.01	0.01				0.10	0.10	
adsorption	⩽ 0.01	⩽ 0.01 [7]	⩽ 0.01 [7]						
impurities	⩽ 0.01	⩽ 0.01 [8]	⩽ 0.01 [8]						
decay scheme (K factor)	0.03	0.03	⩽ 0.01	0.16	0.058	0.22	0.22	0.22 [13]	
half life				0.117	0.32	0.07	0.07	0.07	0.07
dilution factor				0.004 [8]	0.004 [8]				
peak separation				0.45					
N_1						0.2			
N_2						0.3			
detection efficiency									0.10
tail extrapolation									0.20
resolving time									
fitting of extrapol. curve									
accidental summing									
lower level discrim. for N_1									
gate									
accidental coincidence									
after pulse									
spurious pulses									
threshold drift									
satellites									
sum-peak effects									
extrapol. to zero count rate									
source-to-detector distance									
Gandy effect									
other effects									
Combined uncertainty	0.18	0.06	0.05	0.5	0.33	0.5	0.55	0.44	0.34

Table 13 (continued)

Laboratory	CNEN			ENEA	ETL		IEA	KSRI	IMRI
Method*	1	2	4	1	1	3	2	4	2
Components due to:									
counting statistics	0.23	0.20	0.27 [14]	0.08	0.1 [17]	0.4 [26]	0.050	0.21 [31]	0.06
weighing	0.10	0.10	0.03	0.02	0.01 [18]	0.02 [18]	0.030	0.03 [32]	0.03
dead time	0.006	0.002	0.14	0.01		0.02 [27]	0.040	0.02 [33]	0.028
background	0.005	0.008	[6]	0.05	0.01	0.01	0.003	0.002 [34]	0.024
pile-up					0.1 [19]				
timing	0.005	0.005	⩽ 0.05	0.002 [15]		0.05 [28]	0.010	0.01 [35]	0.003
adsorption			⩽ 0.01	0.001	0.01 [20]	0.01 [20]			
impurities					0.01 [21]	0.01 [21]			
decay scheme (K factor)	0.16	0.16	0.12	0.2	0.1 [22]		0.210	0.02	0.07
half life	0.06	0.06		0.08	0.1 [23]	0.1 [23]		0.47	
dilution factor				0.01	0.05 [24]	0.05 [24]			0.0029
peak separation				0.04					
N_1									
N_2									
detection efficiency									
tail extrapolation	0.28					0.45 [29]			
resolving time			0.09				0.06		
fitting of extrapol. curve			0.11					0.22 [36]	
accidental summing				0.1					
lower level discrim. for N_1				0.01 [16]					
gate					0.3 [25]				
accidental coincidence						0.1 [30]			
after pulse						0.3			
spurious pulses									
threshold drift									
satellites									
sum-peak effects									
extrapol. to zero count rate									
source-to-detector distance									
Gandy effect									
other effects									
Combined uncertainty	0.41	0.28	0.36	0.603	0.37	0.69	0.23	0.56	0.11

Table 13 (continued)

Laboratory	NAC				NIM	NIST		NPL	NRC	
Method*	1	2	4	6 [38]	2	1	1bis	3	7	8
Components due to:										
counting statistics	0.103	0.022	0.065	0.32 [39]	0.2	0.08	0.08	0.07	0.05 [53]	0.05 [53]
weighing	0.075	0.075	0.075	0.05	0.06	0.08 [42]	0.15	0.09 [49]	0.05 [54]	0.05 [54]
dead time	0.001	0.005	0.002	0.09	0.01	0.1 [43]	0.05	0.02 [50]	[55]	0.03
background	0.001	0.003	0.019	0.05	0.01	0.005	0.01	0.01	0.02	0.02
pile-up						0.1			0.05	0.05
timing							0.04		0.01 [56]	0.01 [56]
adsorption						0.05 [44]	0.08 [44]	0.01	0.01 [57]	0.01 [57]
impurities						⩽ 0.01	⩽ 0.01	⩽ 0.01 [51]	[58]	[58]
decay scheme (K factor)	0.17	0.12	0.12			0.06	0.13			
half life					0.2	0.02 [45]				
dilution factor					0.06		0.05			
peak separation										
N_1										
N_2										
detection efficiency						0.1 [46]				
tail extrapolation						0.15 [47]				
resolving time		0.023	0.030	0.007				0.05		
fitting of extrapol. curve	0.20			0.40		0.06 [48]		0.26 [52]		
accidental summing										
lower level discrim. for N_1 gate										
accidental coincidence					0.1					
after pulse										
spurious pulses										
threshold drift	0.1									
satellites				0.03						
sum-peak effects					0.5 [40]					
extrapol. to zero count rate							0.05			
source-to-detector distance							0.25			
Gandy effect								0.05		
other effects					0.2				0.4 [59]	0.4 [59]
Combined uncertainty	0.31 [37]	0.145	0.160	0.53	0.6 [40]	0.27	0.35		0.40	0.40
					0.4 [41]					

Table 13 (continued)

Laboratory	O M H	P S P K R			P T B		U V V V R		V N I I M	
Method*	1	1	2	4	1	4	1	2	2	3
Components due to:										
counting statistics	0.03	0.5	0.1	0.3	0.46	0.01	0.041	0.043	0.1	0.1
weighing	0.015 [60]	0.6	0.6	0.6					0.05	0.05
dead time	0.005	0.6	0.5	0.5		0.02 [64]	0.01	0.01	0.05	0.05
background	0.01	0.2	0.2	0.2	0.01	0.02	0.01	0.01	0.1	0.1
pile-up		0.2	0.2	0.2	0.01		0.04		0.05	0.05
timing	0.005	0.2	0.2	0.2	0.01	0.01		0.05	0.05	0.05
adsorption	⩽ 0.001				0.05 [61]	0.05 [61]	0.01 [65]	0.01 [65]	0.02	0.02
impurities	⩽ 0.001				0.01	0.01				
decay scheme (K factor)	0.08						0.10	0.09	0.1	
half life	0.02						0.15	0.15		0.005
dilution factor							0.15	0.15		
peak separation	0.10									
N_1										
N_2										
detection efficiency										
tail extrapolation										
resolving time									0.05	0.05
fitting of extrapol. curve				0.5		0.2				0.3
accidental summing										
lower level discrim. for N_1 gate										
accidental coincidence							0.3			
after pulse										
spurious pulses										0.05
threshold drift										
satellites										
sum-peak effects										
extrapol. to zero count rate	0.1									
source-to-detector distance										
Gandy effect										
other effects		0.6			0.3 [62]	0.3 [62]			0.2	0.4
					0.6 [63]					
Combined uncertainty	0.17	1.20	0.91	1.03	0.8	0.37	0.38	0.24	0.34	0.54

Table 13 (continued)

* The figures in this line refer to the methods used, as listed in paragraph 8 of the Table of contents.

1 Uncertainty in the intercept (at zero mass) of a fit of apparent activity versus mass using the averaged results of 6 sources (the extrapolation accounts for pile-up which is difficult to measure).

2 Possible variation of the estimated average.

3 Internal error in the weighted mean of 153 results.

4 From calibration of balance.

5 Effect of a 1σ variation on the dead time value.

6 Included in counting statistics.

7 From adsorption analysis by Ge.

8 From Ge counting.

9 The external error in the weighted mean of 15 intercepts from 15 individual fits of data for 6 sources ($\geqslant$ 400 points).

10 15 μg per source.

11 Live timing multichannel analyzer.

12 255 data points (fit).

13 K' factor.

14 $(1/N_1 + 1/N_2 + 1/N_c)^{\frac{1}{2}}$.

15 Stability and accuracy of timer.

16 Due to loss of counts for $E \leqslant 10$ keV.

17 Standard deviation of the mean.

18 10 μg uncertainty.

19 10 % of the correction.

20 Adsorption test.

21 γ-ray spectrometry.

22 From decay data evaluation.

23 0.4 day uncertainty.

Table 13 (continued)

[24] Difference of two results.

[25] Setting of the singles-peak region.

[26] Statistics of extrapolation.

[27] 10 % of correction due to the slope.

[28] Gandy effect.

[29] Difference between two results by linear and binomial extrapolation.

[30] 10 % of correction.

[31] Standard error for 7 sources.

[32] $\Delta m/\overline{m}$, where $\overline{m}$ is the mean mass.

[33] Estimated from measured uncertainty.

[34] Estimated from measured count rate.

[35] Inaccuracy of the crystal oscillator.

[36] From limits of least-squares fit for extrapolation.

[37] To account for the error due to random pile-ups, sources of different strengths were made and counted under the same conditions. An extrapolation of the measured activity of the mass solution (as given by each source) was made to zero mass (i.e. zero source activity) to get the correct disintegration rate of the solution.
The following formula was derived to estimate the uncertainty in the disintegration rate of the measured source:

$$\sigma^2(N_o) = \frac{(N_1 + 2\,N_2)^2}{4\,N_2^2}\,\frac{N_1}{t} + \frac{(4\,N_2^2 - N_1^2)^2}{16\,N_2^4}\,\frac{N_2}{t},$$

where t is the counting interval.
Each point was weighted accordingly ($1/\sigma^2$). A linear fit was found.

[38] Method 3, where the proportional counter is replaced by a liquid scintillator.

[39] Standard deviation of 7 measurements.

[40] When the gate includes both the singles and sum peaks.

[41] When the gate includes only the singles peak.

[42] $S = \Delta m/\overline{m}$, where $\Delta m = 20$ μg and $\overline{m}$ is the mean mass.

[43] Live-timer accuracy.

Table 13 (continued)

[44] Adsorption and evaporation.

[45] Decay correction to May 15, 1988.

[46] Efficiency variation in source.

[47] Sum-peak tail.

[48] Extrapolation to zero energy.

[49] Includes dilution and source weights.

[50] Main contribution from τ_β.

[51] Determined by γ spectrometry.

[52] Extrapolation of $N_\beta/\varepsilon_\beta$ versus $(1 - \varepsilon_\beta)/\varepsilon_\beta$ and variation with weight of drop.

[53] Internal uncertainty on combined data.

[54] Precision calibrated balance.

[55] Not required in anticoincidence counting.

[56] Variance on live timing.

[57] Estimated.

[58] Assumed to be pure.

[59] Spread in values observed when changing such conditions as counting gas (Ar + 10 % CH_4 to CH_4) and gamma window, to include sum peak and efficiency extrapolation.

[60] Weighing and dilution.

[61] By experience.

[62] Chemical effects and precipitation. This effect was estimated from the spread of the count rate to mass ratios of the individual sources.

[63] Separation of correlated spectral regions for the analysis of the pulse-height spectrum.

[64] Dead time plus accidental coincidences.

[65] Adsorption and leak.

Table 14 - Main uncertainty components of the final result

Laboratory	Main contributions to the combined uncertainty	Value of the main contributions (%)	Total uncertainty (%)	Method *
AECL	counting statistics	0.14	0.18	1
	timing	0.10		
	counting statistics	0.04		2
	decay scheme "K factor"	0.03	0.06	
	weighing	0.02		
	counting statistics	0.04	0.05	3
	weighing	0.02		
BIPM	peak separation	0.45		1
	counting statistics	0.117	0.51	
	decay	0.117		
	decay	0.32	0.33	2
CBNM	uncertainty from N_2	0.30		1
	decay-scheme correction	0.22		
	uncertainty from N_1	0.20	0.5	
	counting statistics	0.15		
	weighing	0.15		
	counting statistics	0.44		2
	decay-scheme correction	0.22		
	weighing	0.15	0.55	
	dead time	0.10		
	background	0.10		
	timing	0.10		
	counting statistics	0.30		4
	decay-scheme correction K'	0.22		
	weighing	0.15	0.44	
	dead time	0.10		
	background	0.10		
	timing	0.10		
	weighing	0.20		5
	tail extrapolation	0.20		
	dead time	0.10	0.34	
	background	0.10		
	detection efficiency	0.10		

Table 14 (continued)

Laboratory	Main contributions to the combined uncertainty	Value of the main contributions (%)	Total uncertainty (%)	Method *
CNEN	extrapolation	0.28		1
	counting statistics	0.23	0.41	
	decay-scheme correction "K factor"	0.16		
	weighing	0.10		
	counting statistics	0.20		2
	decay-scheme correction	0.16	0.28	
	weighing	0.10		
	counting statistics	0.27		
	dead time	0.14		
	decay correction	0.12	0.36	3
	fitting of extrapolation curve	0.11		
	resolving time	0.09		
ENEA	decay-scheme correction	0.2	0.26	1
	accidental summing	0.1		
ETL	gate	0.3		1
	counting statistics	0.1		
	pile-up	0.1	0.37	
	decay correction	0.1		
	decay-scheme correction	0.1		
	extrapolation	0.45		3
	counting statistics	0.4	0.67	
	after pulse	0.3		
IEA	decay-scheme correction "K factor"	0.21	0.23	2
KSRI	decay correction	0.47		2
	extrapolation	0.22	0.56	
	counting statistics	0.21		
LMRI	decay-scheme correction "K factor"	0.07		2
	counting statistics	0.06		
	weighing	0.03	0.11	
	dead time	0.028		
	background	0.024		

Table 14 (continued)

Laboratory	Main contributions to the combined uncertainty	Value of the main contributions (%)	Total uncertainty (%)	Method *
NAC	fitting of data	0.2	0.31	1
	decay-scheme correction	0.17		
	counting statistics	0.103		
	threshold drift	0.1		
	decay-scheme correction	0.12	0.145	2
	decay-scheme correction	0.12	0.160	4
	fitting of data	0.4	0.53	6
	counting statistics	0.32		
NIM	sum-peak effects [1]	0.5	0.6	1
	counting statistics	0.2		
	other effects (not explained)	0.2		
	decay correction	0.2		
	accidental coincidence	0.1		
NIST	sum-peak tail	0.15	0.27	1
	efficiency variation in source	0.1		
	dead time	0.1		
	pile-up	0.1		
	source-to-detector distance	0.25	0.35	1bis
	weighing	0.15		
	decay-scheme parameters	0.13		
NPL	extrapolation	0.26	0.29	3
NRC	other effects [2]	0.4	0.4	7,8
OMH	peak separation	0.1	0.17	1
	extrapolation to zero count rate	0.1		
PSPKR	weighing	0.6	1.2	1
	dead time	0.6		
	other effects (not explained)	0.6		
	counting statistics	0.5		
	weighing	0.6	0.91	2
	dead time	0.5		
	weighing	0.6	1.03	3
	dead time	0.5		
	extrapolation	0.5		

Table 14 (continued)

Laboratory	Main contributions to the combined uncertainty		Value of the main contributions (%)	Total uncertainty (%)	Method *
PTB		[3]	0.6		1
	counting statistics		0.46	0.8	
		[4]	0.3		
		[4]	0.3	0.37	4
	fitting of extrapolation curve		0.2		
UVVVR	gate		0.3		1
	decay correction		0.15	0.38	
	dilution		0.15		
	decay-scheme correction		0.1		
	dilution		0.15	0.24	2
	decay correction		0.15		
VNIIM	other effects (not explained)		0.2		2
	decay scheme correction		0.1	0.34	
	background		0.1		
	counting statistics		0.1		
	other effects (not explained)		0.4		3
	fitting procedure		0.3	0.54	
	counting statistics		0.1		
	background		0.1		

* The figures in this column refer to the methods used, as listed in paragraph 8 of the Table of contents.

[1] When the gate includes both the singles and sum peaks. In the other case these effects disappear and the total uncertainty is 0.4 %.

[2] Spread in values observed when changing such conditions as counting gas ($Ar+CH_4$ 9:1) to (CH_4) and gamma window, to include sum-peak and efficiency extrapolation.

[3] Separation of correlated spectral regions for the analysis of the pulse-height spectrum.

[4] Chemical effects and precipitation estimated from the spread of the count rate to mass ratios of the individual sources.

Table 15 - Final results

Laboratory and method*		Activity concentration ($kBq\ g^{-1}$) at reference date** (1988-06-15, 00 h UT)		Combined uncertainty ($kBq\ g^{-1}$)		$T_{1/2}$ determined by lab. (d)	
AECL	1	1 413.35		2.54		59.29 ± 0.07	1
	2	1 413.85		0.78			
	3	1 412.05		0.65			
		1 412.80	2	0.57			
BIPM	1	1 425.1		7.21			
	2	1 420.58		4.74			
CBNM	1	1 422.3		7.0			
	2	1 425.8		7.7			
	4	1 443.2	3	6.3			
	5	1 427.9		4.9			
CNEN	1	1 438.9		5.9			
	2	1 434.1		4.0			
	4	1 430.8		5.2			
ENEA	1	1 446.9		3.8		59.38 ± 0.03	4
ETL	1	1 445.2		5.4			
	3	1 461.0		10.0			
IEA	2	1 421.0		3.0			
KSRI	4	1 358.0		7.6			
LMRI	2	1 435.7		1.6		59.90 ± 0.11	5
NAC	1	1 425.0		4.4		59.40 ± 0.05	[19]
	2	1 436.45		2.09			
	4	1 434.83		2.29			
	6	1 447.6		7.6			
NIM	2	1 433.0	6	9.0	6		
		1 430.0	7	5.0	7		
		1 430.7	2	1.3			
NIST	1	1 436.0		3.9			
	1bis	1 429.0	8	5.0			
NPL	3	1 419.6		4.2			
NRC	7	1 438.23		5.78		59.26 ± 0.03	9
	8	1 431.54		5.71			

Table 15 (continued)

Laboratory and method*		Activity concentration (kBq g^{-1}) at reference date** (1988-06-15, 00 h UT)	Combined uncertainty (kBq g^{-1})	$T_{1/2}$ determined by lab. (d)
OMH	1	1 438.7 [10]	2.4	
		1 438.9 [11]	4.3	
		1 438.75 [2]	0.09	
PSPKR	1	1 440.0	20.0	
	2	1 440.0	10.0	
	4	1 430.0	10.0	
PTB	1	1 429.0	11.0	59.39 ± 0.02 [12]
	4	1 427.0	5.0	
UVVVR	1	1 424.9 [13]	1.3	
	2	1 429.95 [13]	0.35	
		1 429.6 [2]	1.3	
VNIIM	2	1 428.6	4.9	
	3	1 441.2	7.7	

* The figures in this column refer to the methods used, as listed in paragraph 8 of the Table of contents.

** Calculated with $T_{1/2}$ = (59.5 ± 0.4) d.

[1] The half life was checked by doing X-X coincidence measurements with three of the VYNS-film sources from the 1987 trial comparison. The present measured activities were compared with those measured in 1987. This gave essentially a two point half-life fit.

[2] This result (and similar ones in this column) is the weighted mean of the results obtained (sometimes using different methods).

[3] For the average slope of this method it was found -1.037 and not -1. This might explain the difference with method 2.

[4] The decay of a ^{125}I source was followed from May 6 to June 23, 1988. 80 activity measurements were made during this period and they gave the result quoted above.

[5] A set of mylar-sandwiched sources prepared for the X-X coincidence method was measured at regular time intervals from May 5 to June 29, 1988, i.e. over a period of time of about one ^{125}I half life. The results were corrected for decay, using successively half-life values of 59.39, 59.5 and 59.90 d. The results obtained with the first two values show a systematic bias, the most important being for the 59.39 d value. The results obtained with the value of 59.90 d are coherent (Fig. 13). It can be noted that a loss of radioactive matter would have favoured low half-life values. The measurements are still going on.

Table 15 (continued)

[6] When the gate includes the singles only.

[7] When the gate includes the singles and the sum peaks.

[8] A value of (1 434 ± 11) kBq g^{-1}) was obtained using calculated efficiencies rather than by a sum-peak analysis. The result is in good agreement with the other values from NIST, but has a larger uncertainty because of the 0.74 % uncertainty in the efficiencies. Only the first value given is shown in Figure 14 and is used for calculating the mean value.

[9] This measurement was performed on 5 ml of solution sealed in an NBS glass ampoule and measured with an NPL (model 671) $4\pi\gamma$ ionization chamber. The measurements covered a time span of about 346 days.

[10] The measurements performed from 1988-06-14 to 1988-06-17 led to this value; it is the only OMH value taken into account in calculating the mean value for all laboratories.

[11] This value is the result of measurements performed from 17 to 20 May, 1988, adjusted to the reference date.

[12] Value obtained in the frame of the trial comparison and published in [20].

[13] Weighted mean of activity measurements obtained with two different dilutions.

Table 16

Mean values (in Bq mg^{-1}) for all methods and all laboratories. (The number of individual results is indicated in parentheses).

Weighted mean value	1 425.6 ± 1.4	(38)
Unweighted mean value	1 429.8 ± 2.6	(38)

Table 17

Mean values (in Bq mg^{-1}) for all methods if the results of the ETL and the KSRI are omitted.
(The number of individual results is indicated in parentheses).

Weighted mean value	1 425.6 ± 1.4	(36)
Unweighted mean value	1 431.0 ± 1.5	(36)

Table 18

Mean values (in Bq mg^{-1}) for the activity concentration determined by methods 1 to 4. The number of laboratories which have used a given method is indicated in parentheses. The results for methods 5 to 8 are given in Table 15.

Method	Weighted mean value		Unweighted mean value
1	1 428.2 ± 2.6	(13)	1 431.9 ± 2.7
2	1 427.9 ± 1.9	(11)	1 428.8 ± 2.4
3	1 412.6 ± 2.4	(4)*	1 433.5 ± 11.1*
4	1 429.7 ± 7.9	(6)**	1 420.6 ± 12.7**

* If the result obtained by the ETL is excluded, the weighted mean is (1 412.4 ± 1.9) Bq mg^{-1} (3) and the unweighted mean (1 424.3 ± 8.7) Bq mg^{-1}.

** If the result obtained by the KSRI is excluded, the weighted mean is (1 433.8 ± 2.0) Bg mg^{-1} (5) and the unweighted mean (1 433.2 ± 2.8) Bq mg^{-1}.

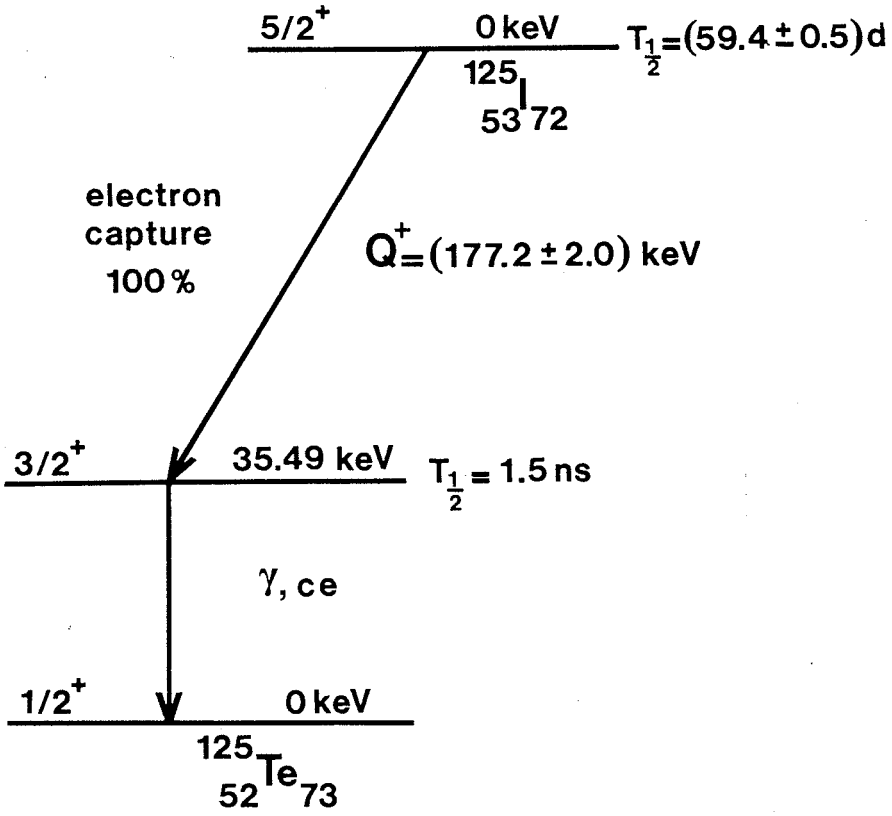

Fig. 1 - Decay scheme of ^{125}I taken from [1].

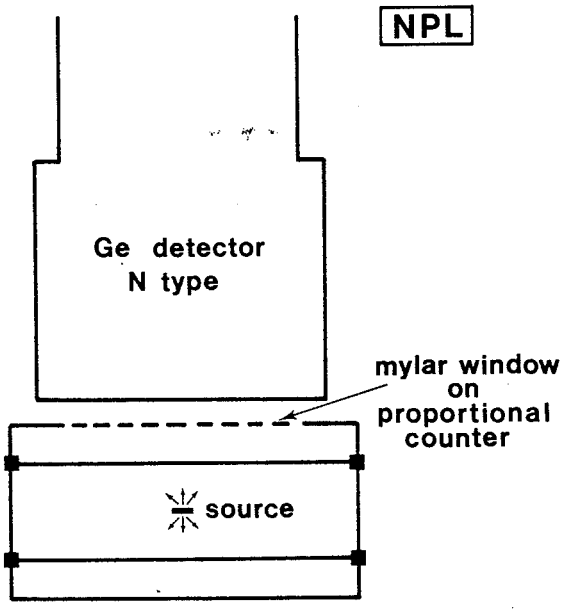

Fig. 2 - Schematic view of the NPL measuring equipment.

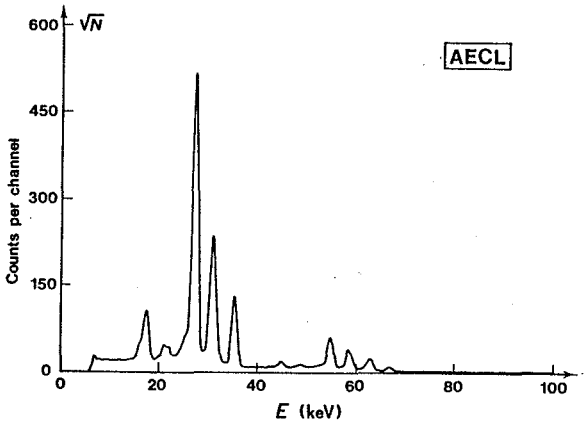

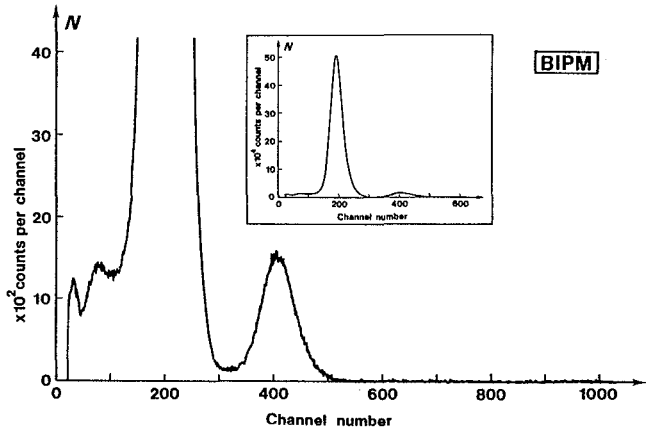

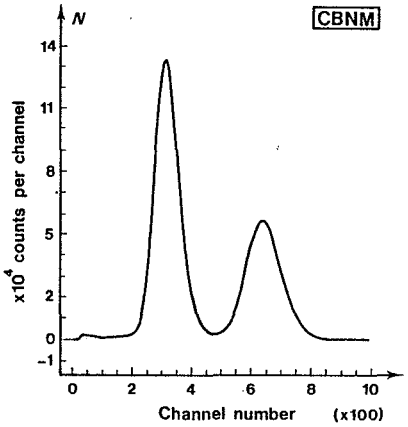

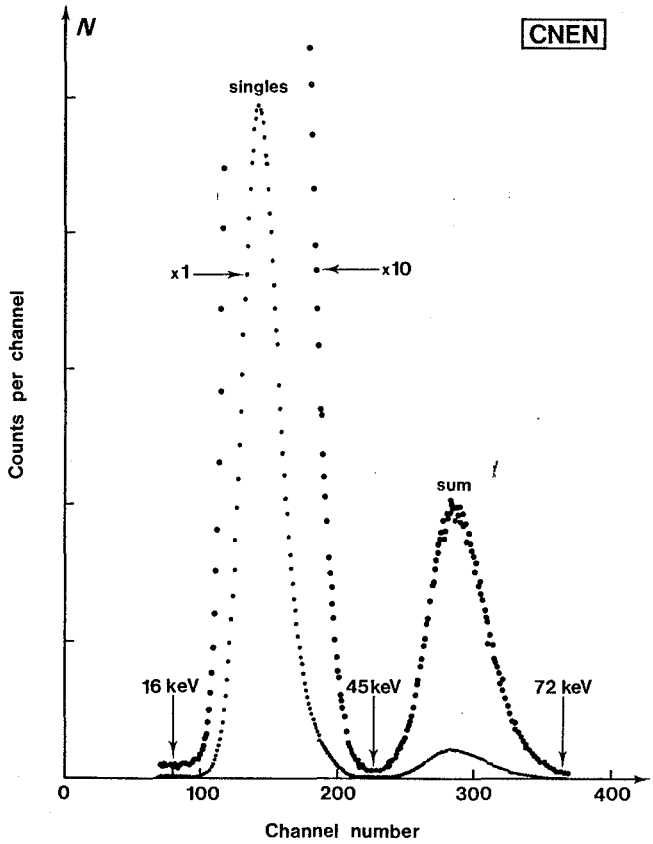

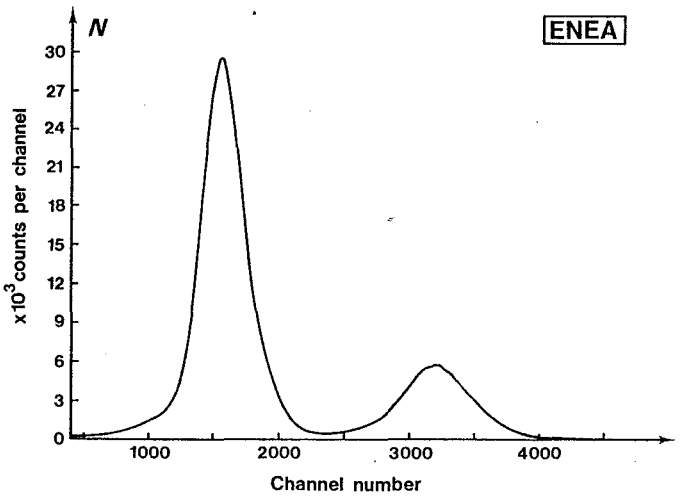

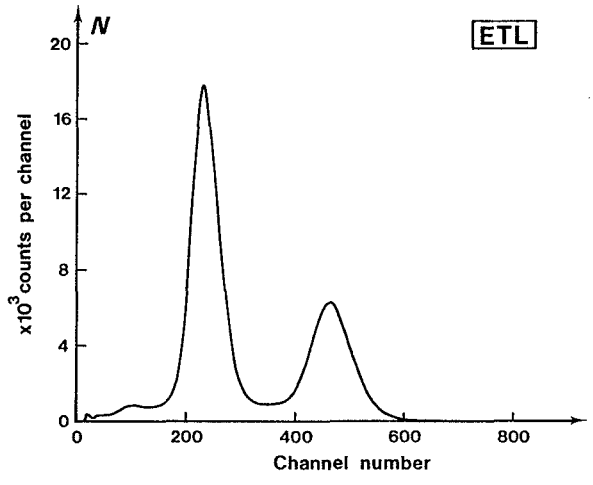

Fig. 3.1 - Typical spectra obtained with method 1. The AECL worked with a Ge detector; all the other laboratories used a NaI(Tl) detector.

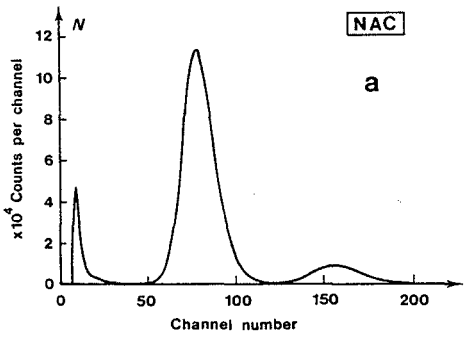

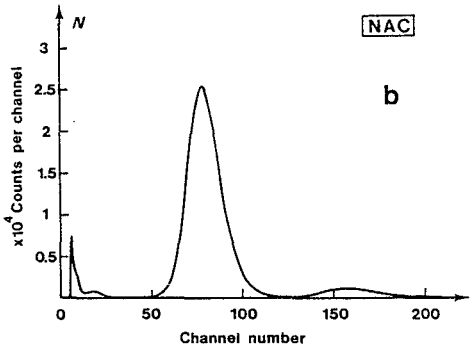

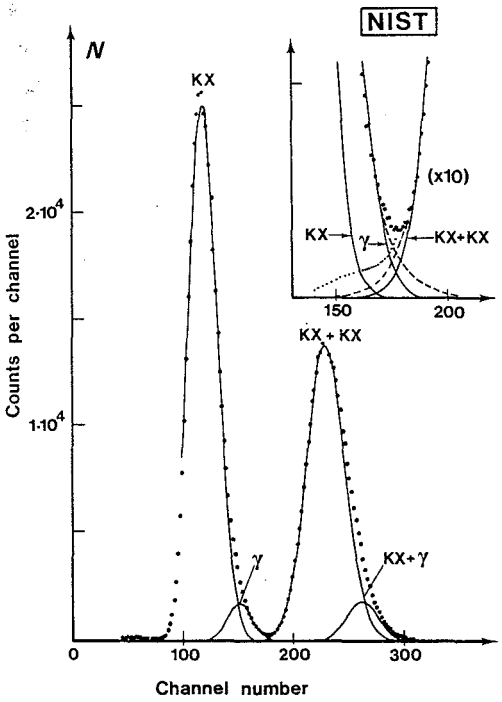

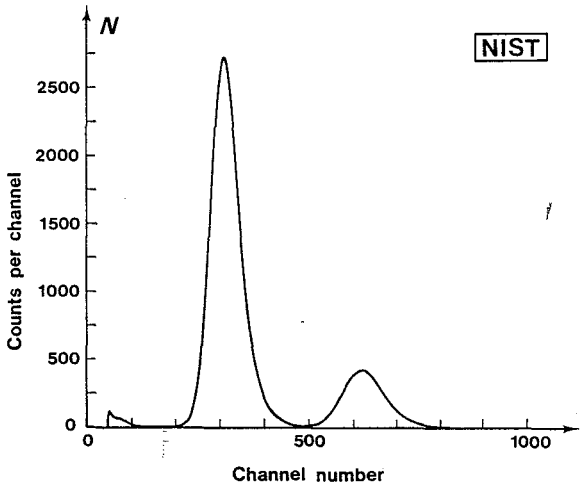

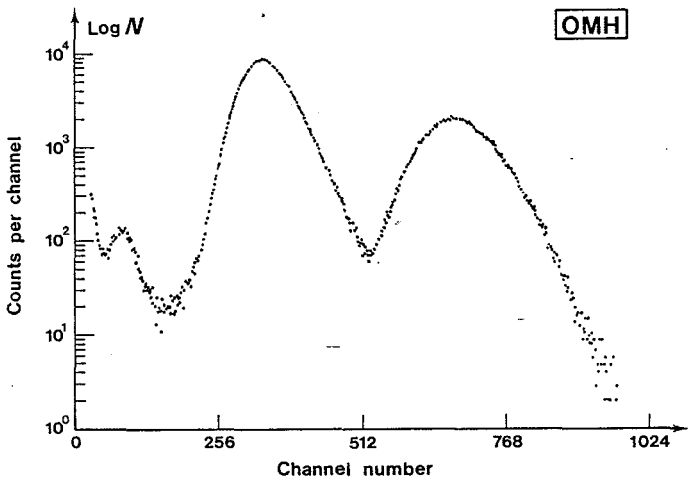

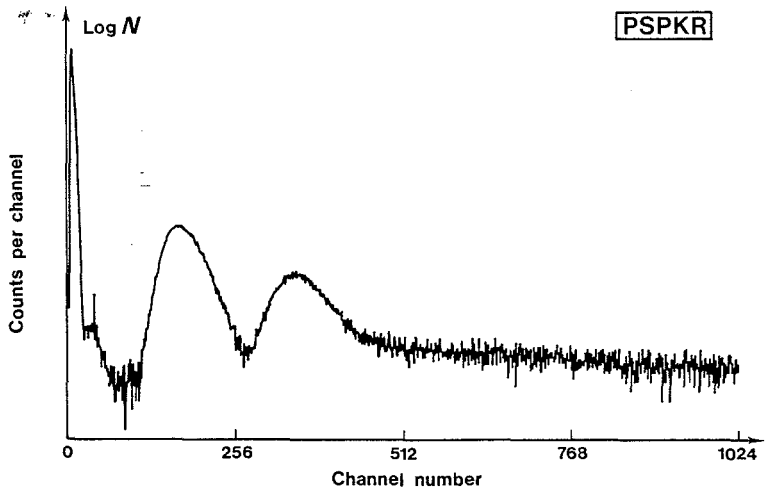

Fig. 3.2 - Typical spectra obtained by means of method 1.
All laboratories used a NaI(Tl) detector. For the NAC, the sources were solid in case a and liquid in case b.

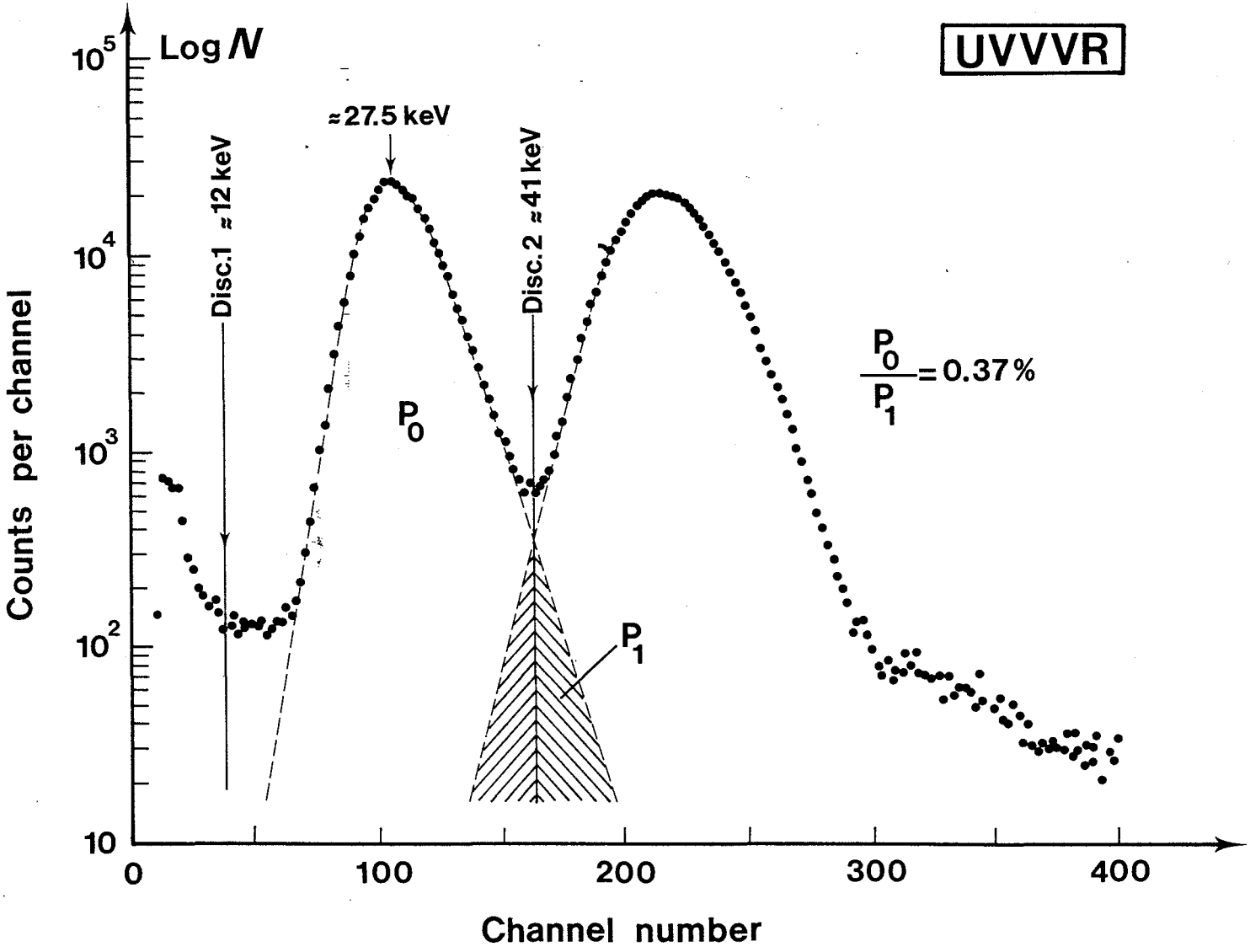

Fig. 3.3 - Typical spectrum obtained at the UVVVR with a NaI(Tl) detector using method 1.

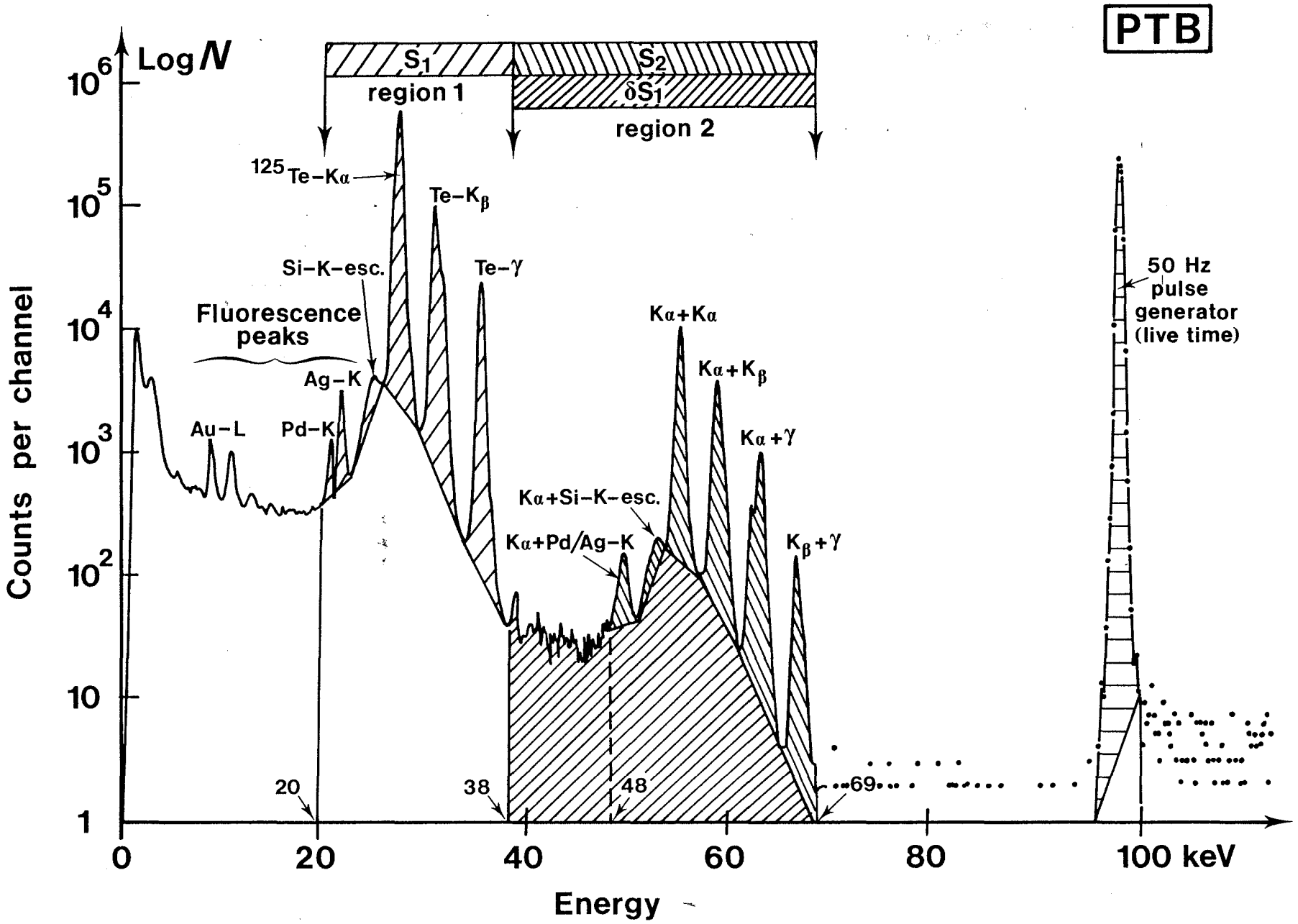

Fig. 4 - Typical spectrum obtained at the PTB with a Si(Li) detector.
S_1, S_2 and δS_1 designate the areas of the corresponding dashed regions and are used in eq. (2).

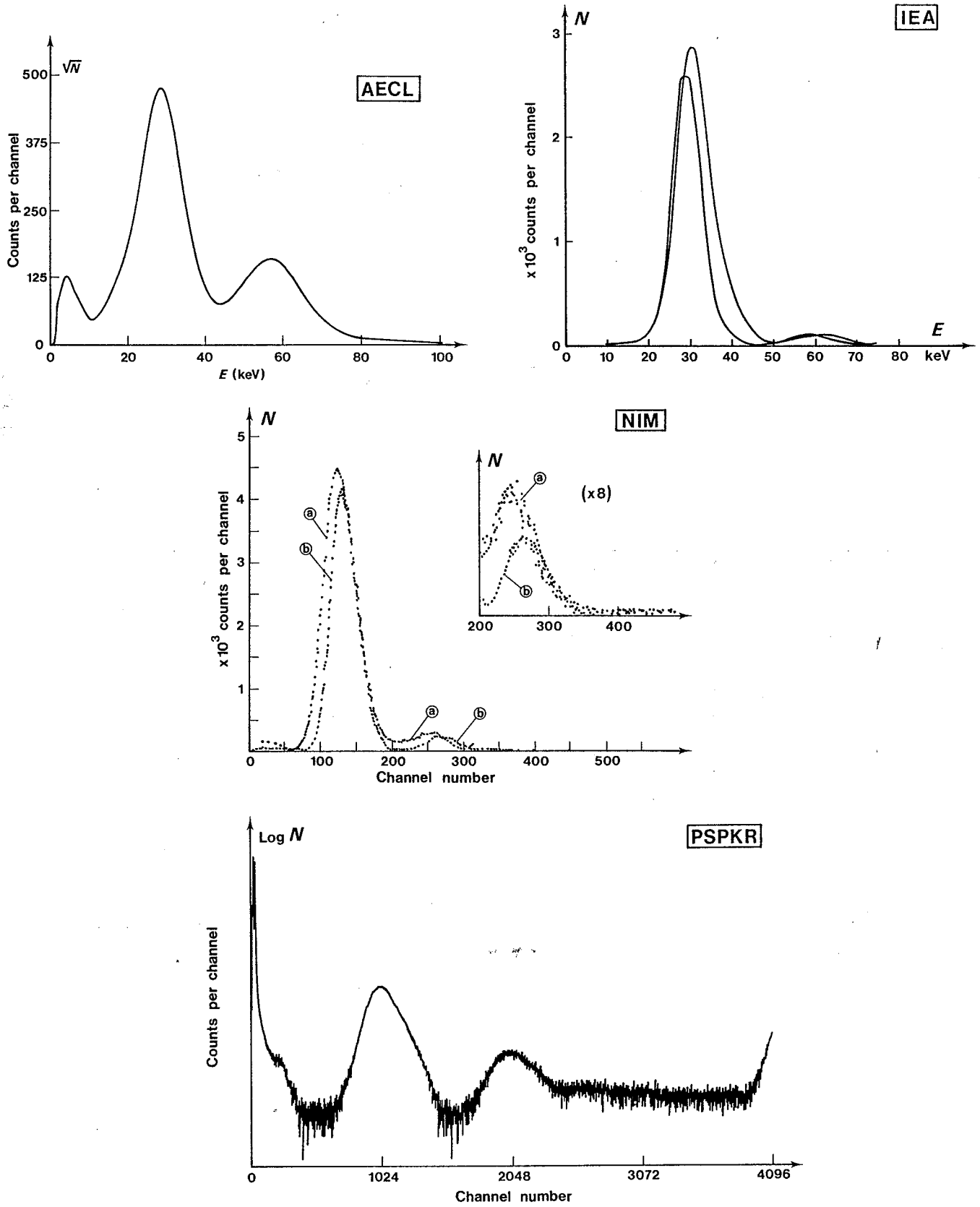

Fig. 5 - Typical spectra obtained by method 2.
In the case of NIM spectra a and b were obtained simultaneously with different detectors.

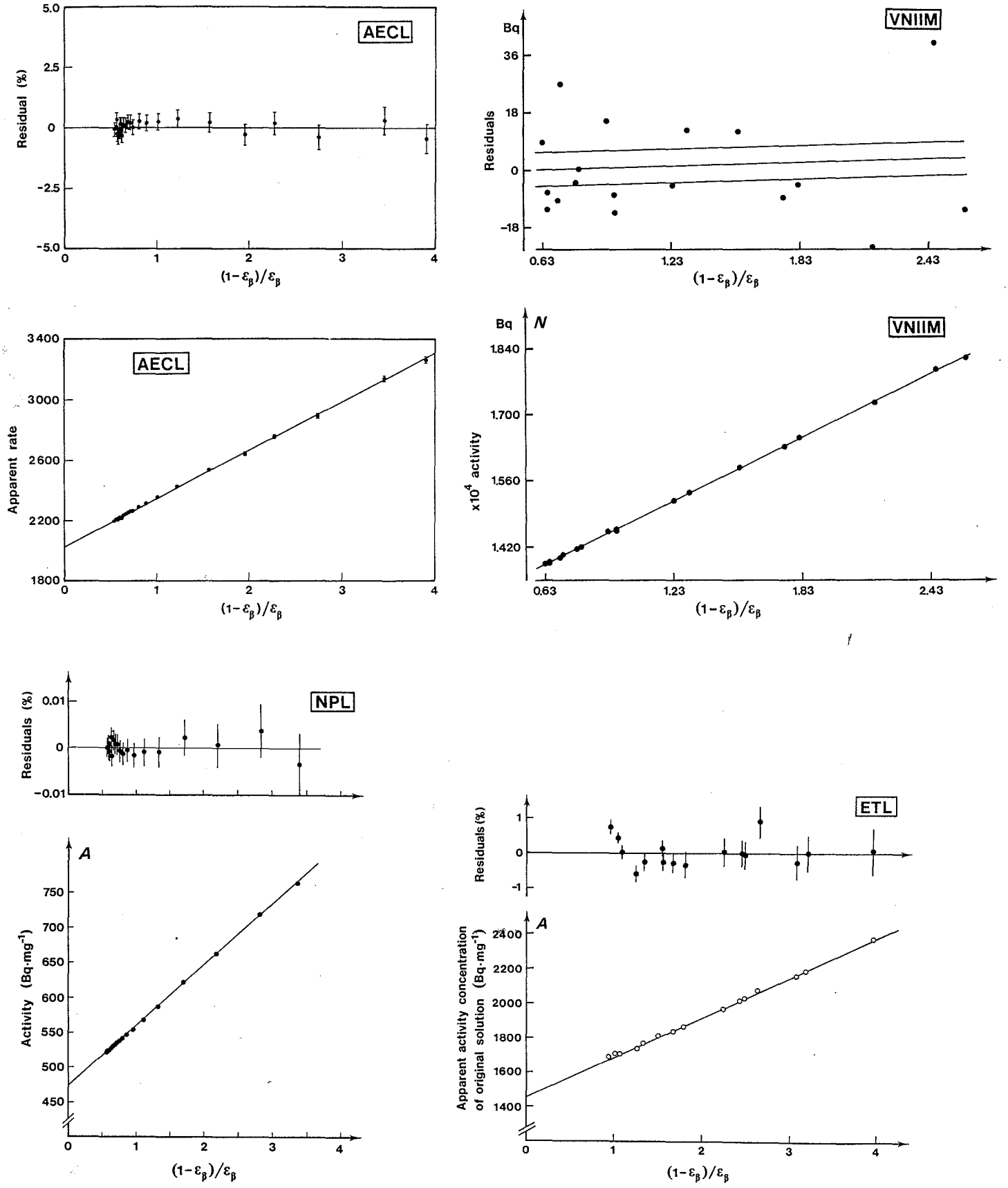

Fig. 6 - Results obtained by the 4πe-X coincidence-efficiency extrapolation method (method 3). For each laboratory the lower drawing presents linear least-squares fit of the activity concentration of the diluted solution versus $(1 - \varepsilon_\beta)/\varepsilon_\beta$. The upper one shows a plot of the residuals for these extrapolations.

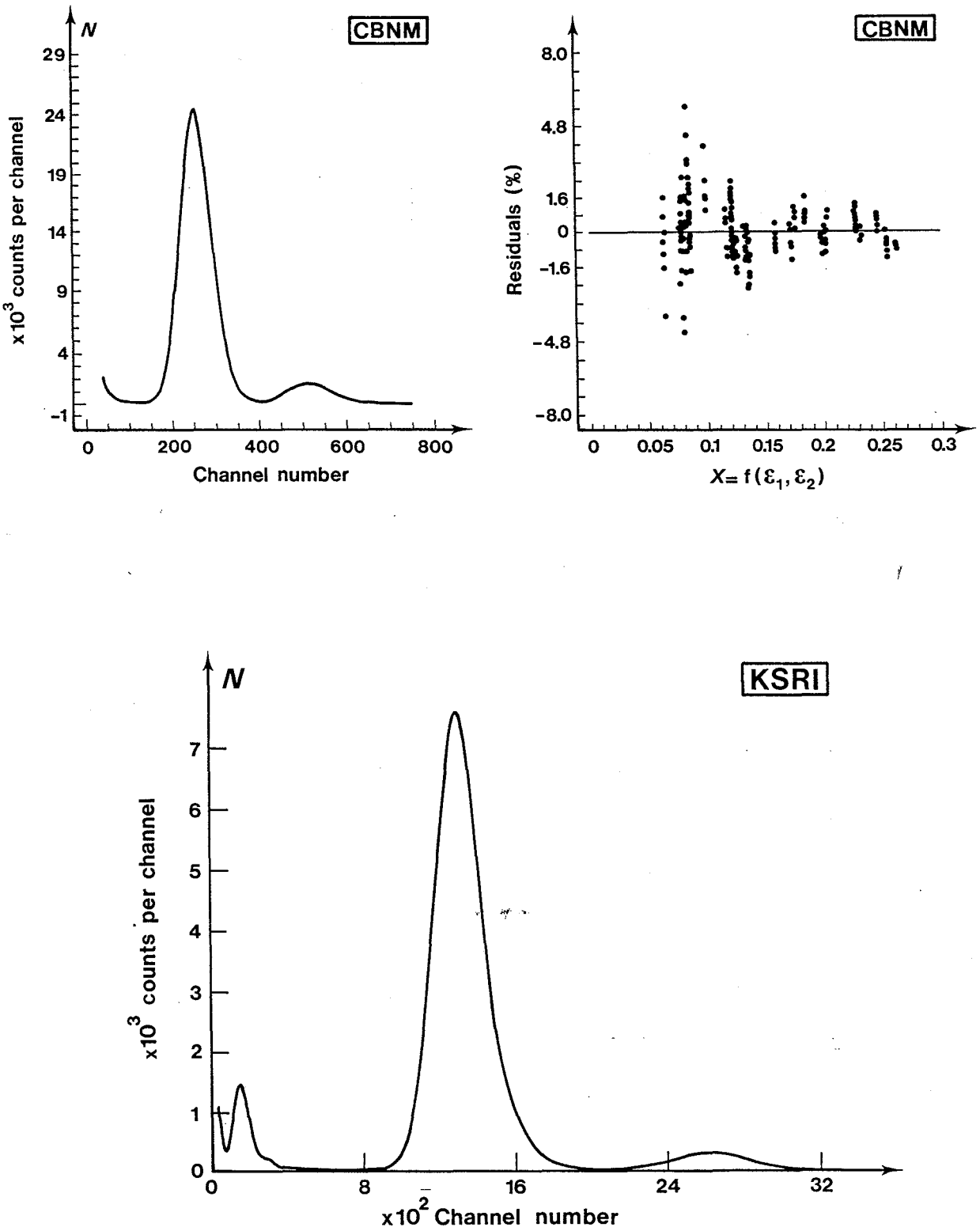

Fig. 7 - Typical data concerning the photon-photon coincidence counting and efficiency-extrapolation method (method 4).

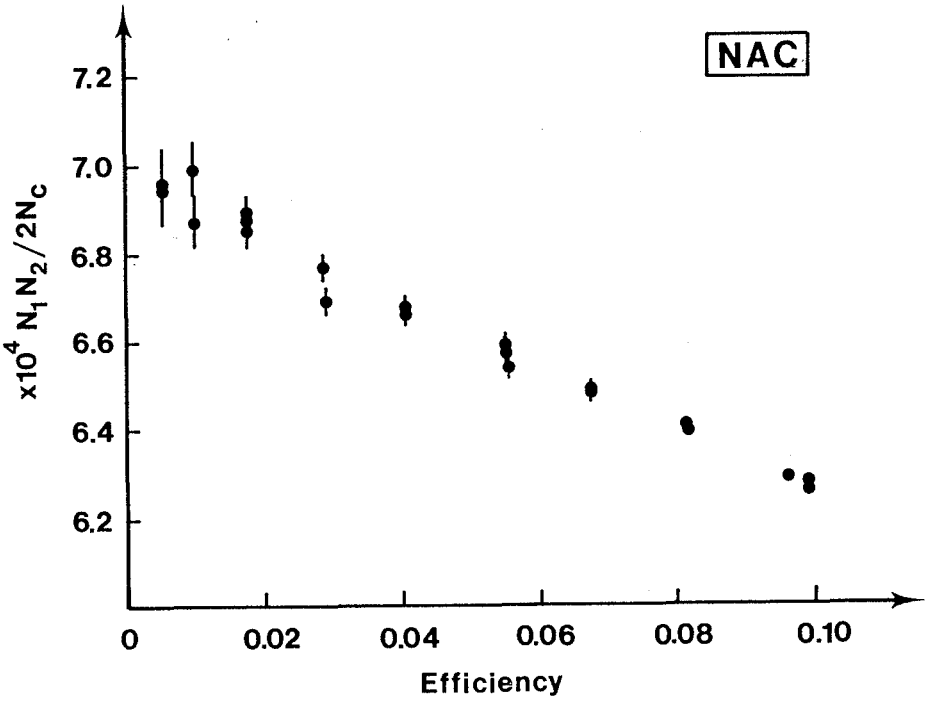

Fig. 8 - Extrapolation of the quantity $N_1N_2/2N_c$ as a function of the efficiency for the photon-photon coincidence counting and efficiency-extrapolation method (method 4) for one of the sources.

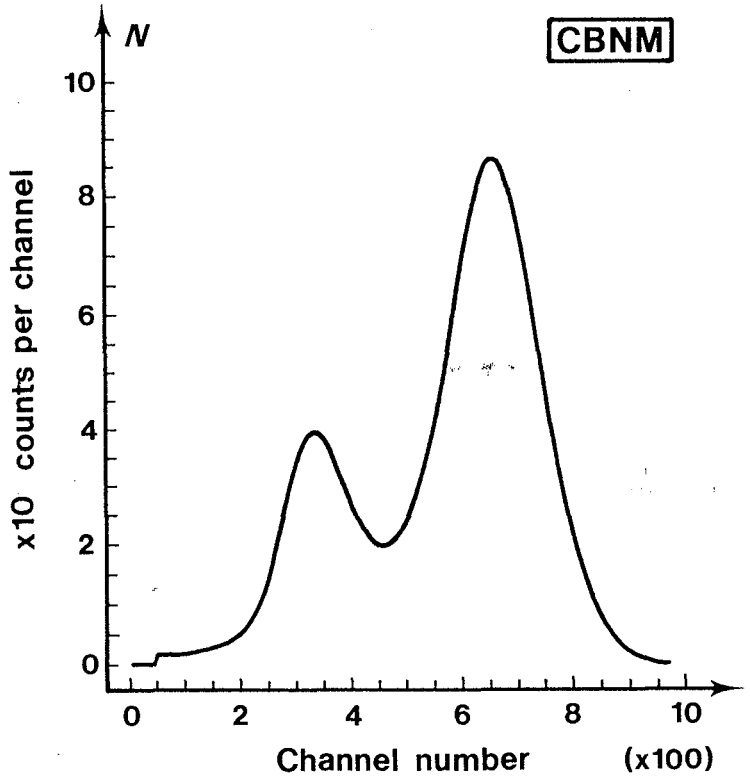

Fig. 9 - Spectrum of ^{125}I obtained by the 4π-CsI(Tl) total counting method (method 5).

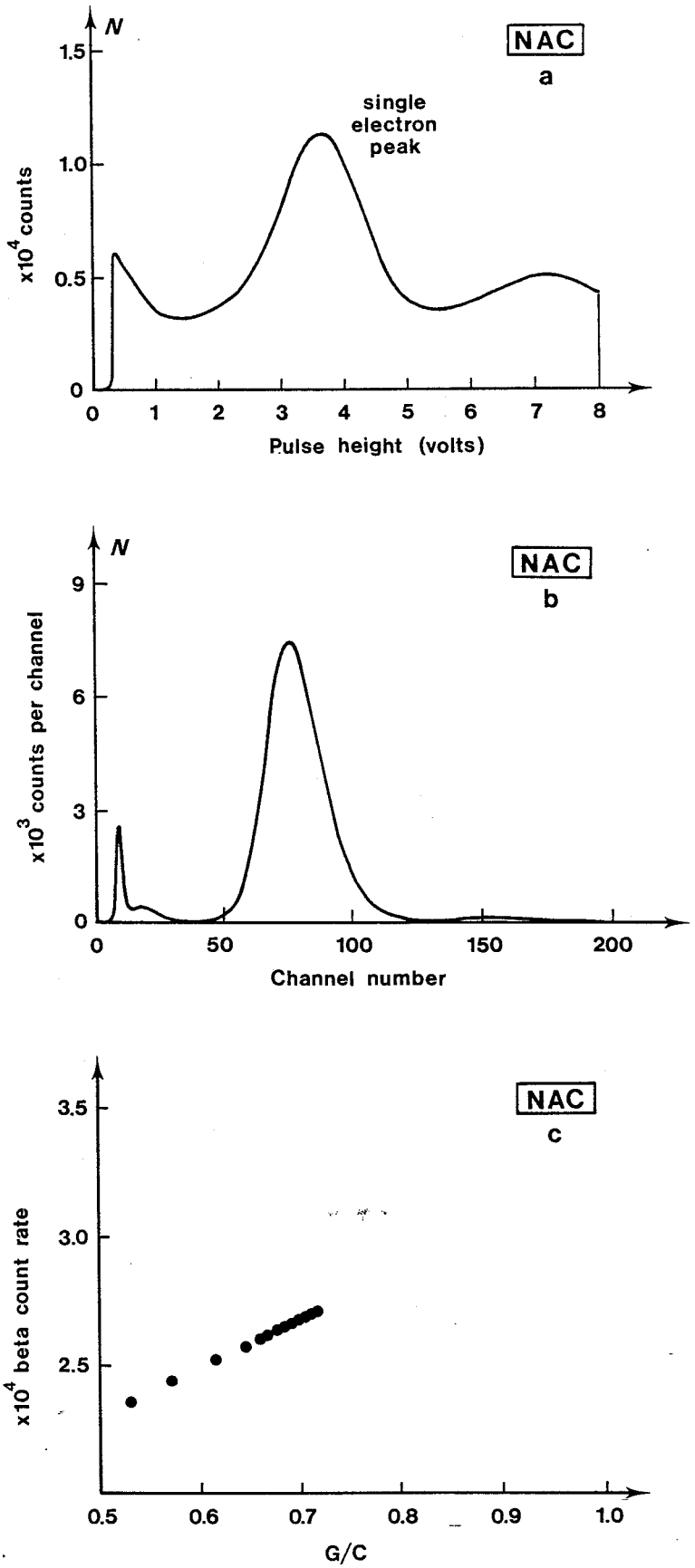

Fig. 10 - Typical data obtained with the 4π(LS)e-X method (method 6). An electron spectrum and an X-ray spectrum are shown in a and b, respectively. In c the count rate is represented as a function of the efficiency.

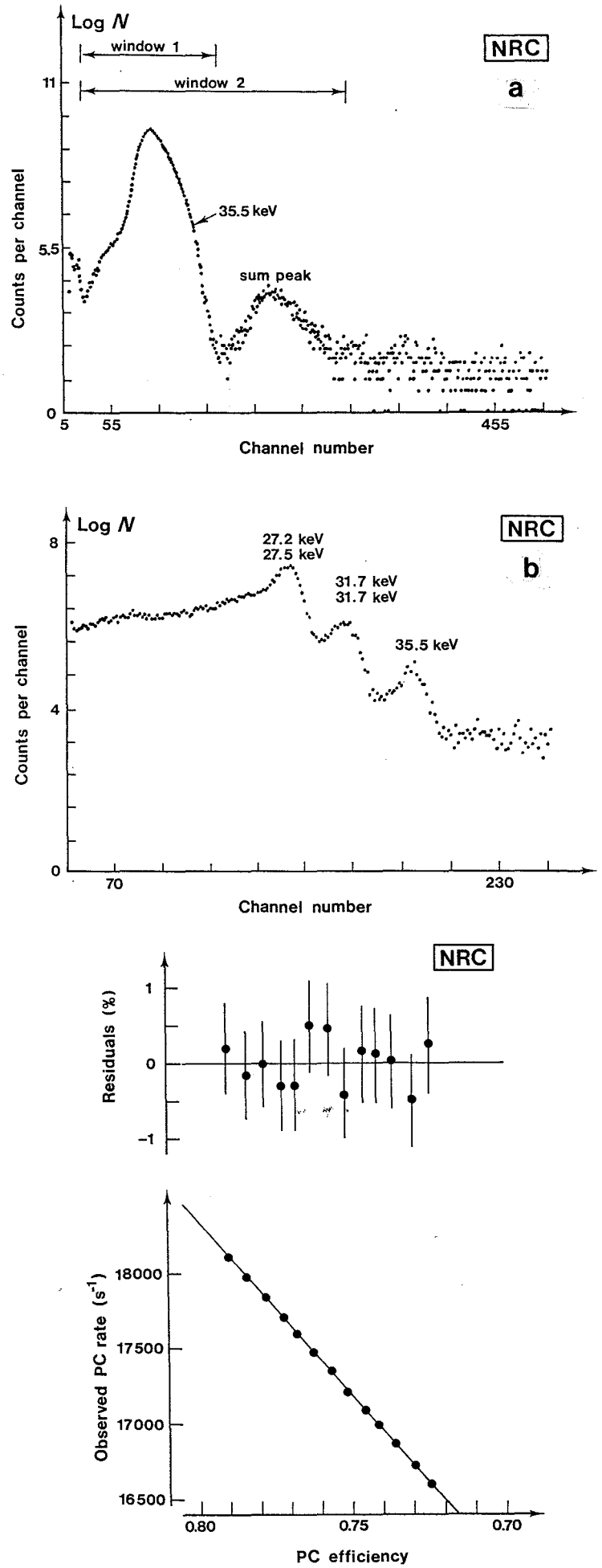

Fig. 11 - Spectra and extrapolation curve obtained with the 4π(PC)e photon-anticoincidence method (method 7). Spectrum a and spectrum b are measured with NaI(Tl) and Ge(Li) detectors, respectively.

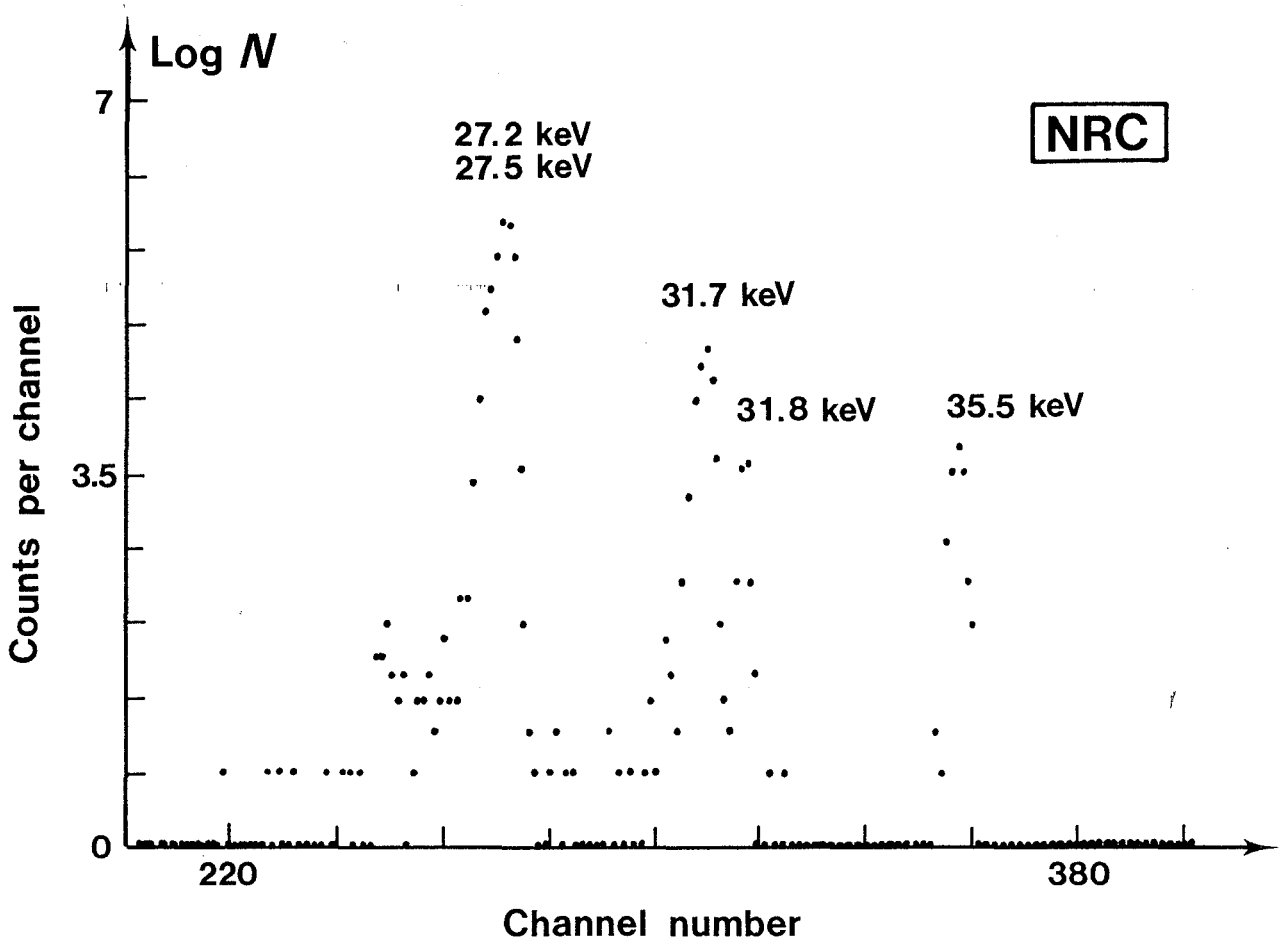

Fig. 12 - Spectrum obtained with a Si(Li) detector by means of the 4π(PC)e photon-coincidence method (method 8).

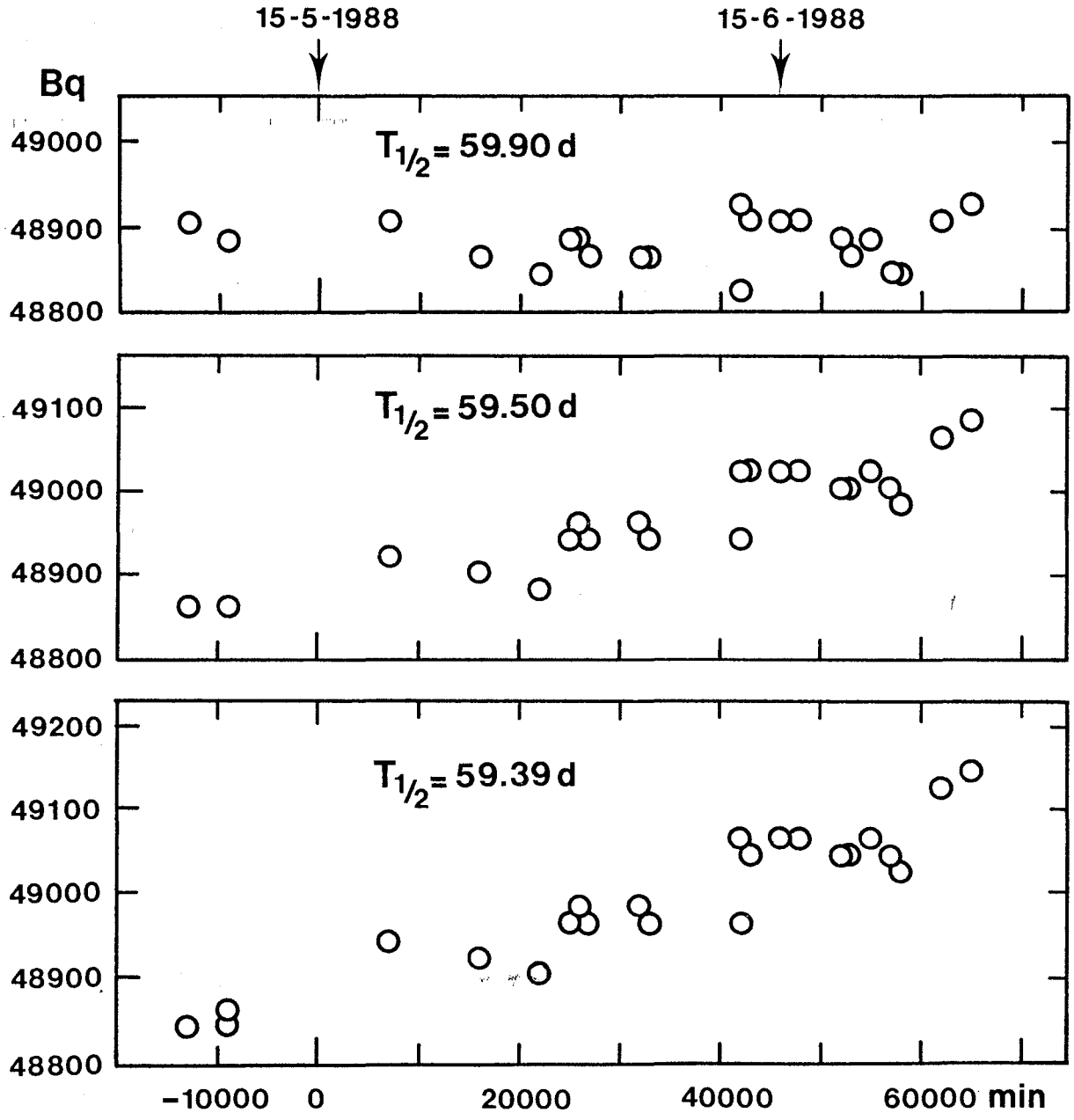

Fig. 13 - Comparison of the results obtained at the LMRI with three different values for the half life of ^{125}I.

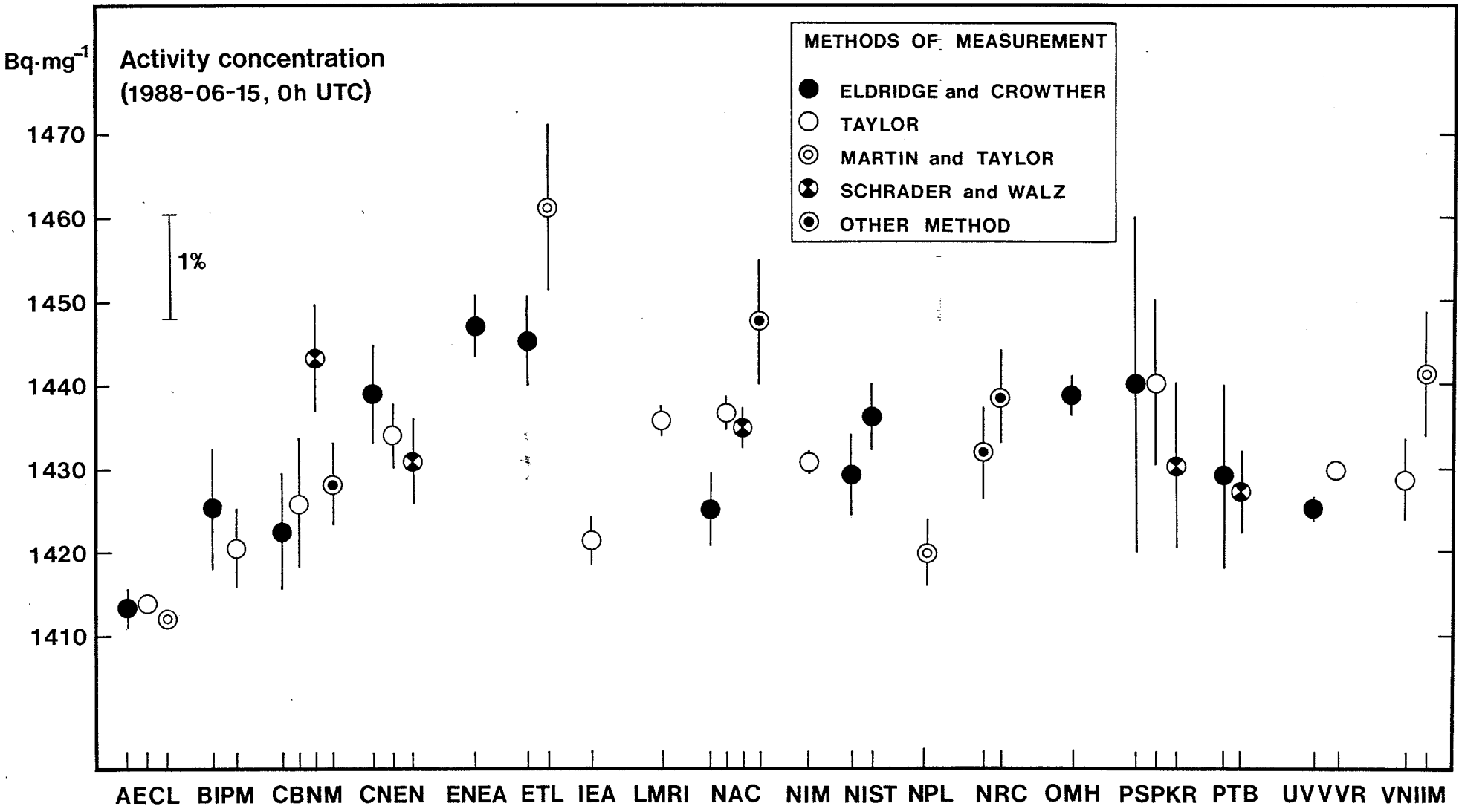

Fig. 14 - Final results of the ^{125}I international comparison.
The value communicated by KSRI (A = 1 358 kBq g^{-1}) is too low and does not appear in the figure.

References

[1] LAGOUTINE F., COURSOL N. et LEGRAND J. Table de Radionucléides, (CEA-LMRI, B.P. 21, F-91190 Gif-sur-Yvette) (The sheet concerning ^{125}I is dated December 1982)

[2] RATEL G. and MÜLLER J.W. Trial comparison of activity measurements of a solution of ^{125}I, final report. Rapport BIPM-88/2, 1988, 22 pages. (Bureau International des Poids et Mesures, F-92312 Sèvres Cedex)

[3] ELDRIDGE J.S. and CROWTHER P. Absolute determination of ^{125}I in clinical applications. Nucleonics 22, 1964, pp. 56-59

[4] MARTIN R.H. and TAYLOR J.G.V. Standardization of ^{109}Cd by a $4\pi e$-X coincidence method. Int. J. Appl. Radiat. Isot. 38, 1987, pp. 781-786

[5] TAYLOR J.G.V. and MERRITT J.S. Branching ratio in the decay of ^{7}Be. Can. J. Phys. 40, 1962, pp. 926-929

[6] DENECKE B. Measurement of the 59.5 keV gamma-ray emission probability in the decay of ^{241}Am with a 4π-CsI(Tl) sandwich-spectrometer. Int. J. Appl. Radiat. Isot. 38, 1987, p. 823-830

[7] NCRP report n° 58. A handbook of radioactivity measurements procedures, 1985 (National Council on Radiation Protection and Measurements, Bethesda, MD)

[8] TAYLOR J.G.V. X-ray-X-ray coincidence counting methods for the standardization of ^{125}I and ^{197}Ag. In Standardization of Radionuclides, Proceedings of a Symposium, Vienna, 1966, pp. 341-354 (IAEA, Vienna, 1967)

[9] SCHRADER M. and WALZ K.F. Standardization of ^{125}I by photon-photon coincidence counting and efficiency extrapolation. Int. J. Appl. Radiat. Isot. 38, 1987, pp. 763-766

[10] IWAHARA A., MARECHAL M.H., DA SILVA C.J. and POLEDNA R. Determination of the activity concentration of a ^{125}I solution by X-(X,γ) coincidence counting and an efficiency extrapolation curve. Nucl. Instr. and Meth. A286, 1990, pp. 370-374

[11] SIMPSON B.R.S. and MEYER B.R. A multiple-channel 2- and 3-fold coincidence counting system for radioactivity standardization. Nucl. Instr. and Meth. A263, 1988, pp. 436-440

[12] SANTRY D.C., BOWES G.C. and MUNZENMAYER K. Standardization of ^{67}Ga by live-timed anticoincidence counting with extending dead time. Int. J. Appl. Radiat. Isot. 38, 1987, pp. 787-791

[13] BAERG A.P. Multiple channel $4\pi\beta$-γ anticoincidence counting. Nucl. Instr. and Meth. 190, 1981, pp. 345-349

[14] COX D.R. and ISHAM V. A bivariate point process connected with electronic counters. Proc. Roy. Soc. A356, 1977, pp. 149-160

[15] BRYANT J. Coincidence counting corrections for dead-time loss and accidental coincidences. Int. J. Appl. Rad. Isot. 14, 1963, pp. 143-149

[16] CAMPION P.J. The standardization of radioisotopes by the beta-gamma coincidence method using high efficiency detectors. Int. J. Appl. Radiat. Isot. 4, 1959, pp. 232-248

[17] SMITH D. Improved correction formulae for coincidence counting. Nucl. Instr. and Meth. 152, 1978, pp. 505-519

[18] GIACOMO P. News from the BIPM. Metrologia 17, 1981, pp. 69-74

[19] SIMPSON B.R.S. and MEYER B.P. The half-life of ^{125}I. Technical Note, Int. J. Appl. Radiat. Isot. 40, 1989, pp. 819-820

[20] SCHRADER H. Measurement of the half-lives of ^{18}F, ^{56}Co, ^{125}I, ^{195}Am and ^{201}Tl. Int. J. Appl. Radiat. Isot. 40, 1989, pp. 381-383